

Journal of Statistics Applications & Probability An International Journal

http://dx.doi.org/10.18576/jsap/110117

Stochastic Modelling of the BRICS Equity Markets' Risks

Rosinah M. Mukhodobwane^{1,*}, Caston Sigauke², Wilbert Chagwiza¹ and Winston Garira¹

Received: 9 May 2020, Revised: 26 Aug. 2020, Accepted: 3 Sep. 2020

Published online: 1 Jan. 2022

Abstract: Effective modelling of extreme financial losses is a key investment strategy required by investors for successful assessment of risk in any financial market. This study compares the modelling capabilities of two extreme value theory (EVT) models via the conditional extreme value's (CEV's) GPD (generalized Pareto distribution) and point process for risk management and risk forecasting in the BRICS (Brazil, Russia, India, China and South Africa) equity markets. Prior to the application of the two EVT models, heteroscedasticity in the BRICS returns was filtered out using the generalized autoregressive conditional heteroscedasticity (GARCH) model. The findings reveal that under the GPD model, the risks in the five BRICS equity markets can all be modelled by the Gumbel class of distributions. Under the point process approach however, the risk in the Russian equity market can be modelled by the Fréchet-Pareto class of distributions, while the risks in the Brazilian, Indian, Chinese and South African equity markets can be modelled by the Weibul class of distributions. Furthermore, in terms of risk levels, the findings show that the Russian IMOEX market is the most risk-prone, while the least risky is the Indian NIFTY market, with the remaining three markets in between them. That is, the Russian IMOEX market has the highest level of risk, followed by the South African JALSH market, then the Chinese SHCOMP, Brazilian IBOV and Indian NIFTY markets, respectively.

Keywords: Conditional extreme value model, Equity markets, Equity risk, GARCH model, Point process approach, Return levels, Risk management

1 Introduction

After series of global financial crises to date, empirical researchers are coming up with continuous modelling of extreme events associated with risk in the financial field. More especially, investors and traders are deeply concerned with daily activities and any unusual or rare movement in the markets where investment and trading occur. The word BRICS is a bloc of five leading emerging regional economies of Brazil, Russia, India, China and South Africa. The BRICS are developing nations with high potentials and comparative good economic performance regionally and globally [1]. In particular, the four BRIC (Brazil, Russia, India, and China) markets are considered the largest and fastest growing economies among the global emerging markets and are also reputed in the literature as the global economic growth's engines [2]. With track of time and globalization, emerging financial markets get bigger and are becoming more developed, hence investors are showing more interest and better attractions to them [3].

Risks are adverse market movements that are of major concern to investors and risk managers. The practice of advanced detection of risks, analysing them and taking preventive measures to alleviate the risks is known as risk management. Financial risks are posed by rare or extreme events existence at the tails of the returns' distributions and the behaviour of an investment portfolio during a financial crisis is an important element of risk management. The study of risk in the tails of equity returns is a crucial area in stock markets research because the general view about investing is that the future could either yield good profits or worrisome losses as an aftermath of investment. Rare events may materialize as large negative or positive investment returns, major defaults, the collapse of risky asset prices, or a stock

Because of the rising need for financial risk management and the series of global financial crisis, forecasting of risk has become a critical issue for stakeholders in basically all finance markets across the globe. The traditional approach used

¹Department of Mathematics and Applied Mathematics, University of Venda, Private Bag X5050, Thohoyandou 0950, Limpopo, South

²Department of Statistics, University of Venda, Private Bag X5050, Thohoyandou 0950, Limpopo, South Africa

^{*} Corresponding author e-mail: rosinah.mukhodobwane@univen.ac.za



for modelling risk was through the use of the value-at-risk (VaR) and expected shortfall (ES) methods, whose concepts are based on the normal distribution assumption. Furthermore, this traditional VaR's estimates are based upon the concept of homoscedasticity, which assumes that the standard deviation of returns does not change over time. Because of this, Engle [4] claims that a much better estimates can be obtained from models that are explicitly based on the concept of heteroscedasticity, which allows the standard deviation to change over time [5].

As opposed to the "normal" concept, financial returns are known to exhibit fat tails and normal distribution cannot effectively model such return's behaviour. Fat tails in the financial returns indicates that extreme outcomes take place much more frequently than what the normal distribution assumption can predict [6]. The deficiency of the VaR and ES models, due to their normal assumption, can be modified using an extreme value theory (EVT) based method of VaR approach [7]. Modelling of risk using model frameworks with a normal distribution assumption are known to understate the result originating from data like the financial returns with fat tails [5],[8], [9].

It has been argued by several authors like de Jesus et al. [10], Santos et al. [11], and McAleer et al. [12] that extreme events contained in the tail distribution of losses can be taken into account explicitly by extreme value theory [13]. As an advantage over classical approaches, the EVT is a parametric method which allows for extrapolation of the tail behaviour to extreme levels. Furthermore, the EVT method does not use the whole dataset but limits it modelling approach to the tail behaviour of a loss distribution using only extreme values [13].

Karmakar and Paul [6] used the two-stage GARCH-EVT approach of McNeil and Frey [14] to model the tails of (return) distributions and compute intraday VaR and ES measures for 16 stock markets across North America, Africa, Asia, Europe, Latin America and Australia. The authors [6] compared the efficacy of the conditional EVT method with other competing models and observed that EVT outperformed the others. McNeil and Frey used the GARCH model to filter the return series to get a nearly i.i.d. (independent and identically distributed) residuals (in the first stage), and they fitted EVT model on the standardized residuals in the second stage [6].

Several other authors have used GARCH-EVT joint approach with other models on various data sets and have observed that the GARCH-EVT method performed better than the competing models (for VaR estimation) when compared. GARCH-EVT model was used by Marimoutou et al. [15], Ghorbel and Trabelsi [16], Cotter [17] etc. to measure VaR in various markets and they observed that the EVT did better than other well-known modeling techniques in forecasting of VaR's estimates [6]. Bali and Neftci [18] applied the duo of a Student's *t* distributed GARCH model and the GARCH-EVT model to U.S. short-term interest rates and the authors discovered that more accurate estimates of VaR were yielded by the GARCH-EVT model than did the Student's *t* distributed GARCH model. Karmakar and Shukla [19] also compared the accurateness of GARCH-EVT method for calculating VaR with other rival models using data from 6 global emerging and developed equity markets. Their findings showed that GARCH-EVT method performed best in the estimation of VaR.

In another study, the point process approach of extreme value models was used by Smith [20] to model the daily returns for General Electric, Pfizer and Citibank from 1982 to 2001. Volatility was first filtered from the data using GARCH(1, 1) model, after which the returns were modelled to analyse the VaR (value at risk). The researcher resolved that in order to obtain a satisfactory extreme value modelling outcome, it is better to remove heteroscedasticity and short-range serial correlation from the return before applying extreme value theory (EVT) models. Many EVT and GARCH based models were estimated by Ergun and Jun [21] to predict intraday VaR for the returns of S & P 500 equity index futures. The researchers' findings showed that the EVT-GARCH based models which take into account conditional kurtosis and skewness provide accurate forecast of VaR. Chavez-Demoulin and McGill [22] used EVT-Hawkes process to measure high frequency intraday VaR. The authors observed that a suitable estimate of high quantile risk measures for the U.S. market's financial time series was provided by the process.

This study applies the GARCH-EVT approach to model financial risk in the BRICS stock markets. The GARCH model will be used to filter out heteroscedasticity in the returns, while the univariate EVT via the conditional extreme value (CEV) model and the point process approach will be used to model the risk in each of the markets. To the best of the authors' knowledge, no study has been done on modelling the BRICS equity markets' risk and even more so, none has been done using the application of these two proposed EVT models.

In statistics and econometrics, probabilities of left tail are closely associated with the likelihoods of extreme downward movements in the market [23]. Even though both the "gains (i.e. positive or right tails)" and "losses (i.e. left or negative tails)" of equity return distributions are of invaluable modelling interest from a risk management point of view, much more studies on extreme equity returns have focused on losses when compared to gains, and large booms are usually considered less important than large crashes [6]. This study focuses on modelling the losses or negative tails of the distribution of the BRICS equity markets. This is because the left tail is of more interest from a risk management viewpoint [24], and a more practical risk measure should be related to large adverse movements, or large losses in the market [25]. For the rest of the paper, Section 2 discusses the models applied, Section 3 presents the empirical analyses and findings, and Section 4 gives the conclusions.



2 Models

To ensure a comprehensive understanding of the statistical theories of EVT models, this study begins with the description of the two fundamental approaches involving the traditional block maxima method (BMM) and the peaks-over-threshold (POT) method. The peaks-over-threshold (POT) method is tailored down to the conditional extreme value (CEV) model and the point process approach since both methods are based on the choice of a reasonably high quantile threshold.

2.1 Block maxima method

With block maxima model, extreme losses are divided into identical blocks where maximum loss in each block is the largest observation. This procedure is termed "block maxima" with each local block containing maximum loss. Thus, the extreme losses can be characterized by the local block maxima which are the data to be fitted or modelled using this method. The generalized extreme value distribution (GEVD) as stated in equation (1) is the asymptotic approximation of the block maxima observations [26,27].

$$G_{\xi}(x) = \exp\left[-\left(1 + \xi \frac{x - \mu}{\sigma}\right)_{+}^{-\frac{1}{\xi}}\right] \tag{1}$$

for
$$\{x|1+\xi\left(\frac{x-\mu}{\sigma}\right)>0\}$$
,

where ξ , μ and $\sigma > 0$ denote the tail shape parameter, the location parameter representing the center of the distribution, and scale parameter (i.e. the size of the deviations about μ) respectively.

In risk management analysis, the distribution of the block maxima has a light tail with finite upper bound for the Weibull distribution, an exponential tail (that is unbounded) for the Gumbel distribution and a heavy tail that includes polynomial decay with no upper limit for the Fréchet distribution [28]. As a limitation, the block maxima method can miss out some of the required high realizations and retains some lower (central) ones [29]. For this reason, preference is usually given to the peaks over threshold (POT) method because it uses all necessary high realizations, which makes it more reliable.

2.2 Peaks over threshold approach

This approach can be described by defining an extreme event as a value that exceeds a high enough threshold and uses only excess observations (i.e. peaks or exceedances) above the threshold for statistical inference. Every point over the chosen threshold is considered an extreme observation set aside for risk modelling. This method is demonstrated under two categories of threshold selection models: the conditional extreme value (CEV) and point process (PP). The limiting distribution of the first model is the generalized Pareto distribution (GPD) while the second model can be approximated by a non-homogeneous Poisson distribution.

Semi-parametric models and fully parametric models are the two analytical frameworks that use POT class of models. The former is built around the Hill estimator and other related estimators [30], while the latter is based on the GPD or generalized Pareto distribution [31]. When applied correctly, both methods are equally relevant but this study will prefer the use of the fully parametric style because it is easier to estimate using the maximum likelihood approach (see Coles [29] for details).

2.3 The conditional univariate extreme value model

The univariate version of the conditional extreme value (CEV) model fits the GPD to marginal variables [32]. Hence, the GPD will be fitted to exceedances above a selected threshold for each of the BRICS markets [29].

2.4 Threshold-excess model

Given that the family of a class of approximating distribution to the tail of an arbitrary distribution function F of a random variable X is

$$G(x) = 1 - \eta \left[1 + \xi \left(\frac{x - u}{\sigma_u} \right) \right]^{-\frac{1}{\xi}}, \quad x > u, \tag{2}$$



where $\xi \neq 0$, $\eta = \Pr(X > u)$, and $\sigma > 0$ for a family defined on $\{x - u : x - u > 0 \text{ and } (1 + \xi(x - u)/\sigma_u) > 0\}$. This indicates that for a sufficiently large threshold, and on the condition that an individual observation exceeds the threshold u (i.e. x > u), $F(x) \approx G(x)$ with parameters η , ξ , and σ [29].

2.5 Threshold selection

In order to select a sufficiently high threshold for the univariate risk modelling, cautious trade off between bias and variance must be ensued. This is necessary to avoid having too high threshold with few realizations with which to make inferences [33], and which can also result in increase of the variance of the parameter estimate because of the reduced sample [34], or too low threshold to avoid bias where non-extreme or central observations are selected in place of extreme ones. In practice, the threshold is required to be suitably high to ensure a reliable asymptotic GPD approximation, hence reducing the bias [35]. This study applied two threshold selection approaches via the "extreme value mixture models" (see [34], [35]) and "threshold stability plot" (see [34], [36]).

2.6 Point process

Like the GPD approximation to excesses above high thresholds, the point process can equally be used to describe exceedances over a sufficiently high threshold. A region is described above the selected threshold such that points in the region signify the extreme events or risk for modelling. The point process approach incorporates other EVT models including the r largest order statistics, the block maxima and the threshold excess models. The development of these EVT models is a result of the representation of the point process, which forms a good reason for considering the approach [29].

The technique of a point process on a set \mathbb{K} is a stochastic approach for the existence and position of events represented as points that are randomly distributed in space. This process can be used to describe the behaviour of extreme events concentration at the tails of the markets, where \mathbb{K} denotes a time period. For each of the selected markets (random variables), a set of non-negative integer values N(K) can be defined such that $K \subset \mathbb{K}$. N(K) is the number of points (events) in each set K and it signifies the number of events, like stock market crashes, that can occur within a specified period of time.

Furthermore, let the intensity measure of the process be defined as

$$\Phi(K) = E\{N(K)\}. \tag{3}$$

This is the average number of events or points in any given subset $K \subset \mathbb{K}$. Also, the derivative function of the intensity measure, with the assumption that $K = [k_1, x_1] \times ... \times [k_p, x_p] \subset R^p$, defines the intensity function of the process as

$$\lambda(x) = \frac{\partial \Phi(K)}{\partial x_1 \cdots \partial x_p}.$$
 (4)

The point process models can be applied statistically by estimating the process using a set of observed events (points) x_1, \ldots, x_n in an interval or a specified region \mathbb{K} . Traditionally, the one-dimensional homogeneous Poisson process is the canonical point process and it is a process on $\mathbb{K} \subset \mathbb{R}$ with a $\lambda > 0$ parameter [29] where it satisfies the following:

- 1. $N(K) \sim \text{Poi}(\lambda(h_2 h_1)) \ \forall K = [h_1, h_2] \subset \mathbb{K}$. Here, the number of events in a specified interval N(K) follows a Poisson distribution whose mean λ is proportional to the length of the interval $(h_2 h_1)$.
- 2. The number of point events, say $N(K_1)$ and $N(K_2)$ taking place in different intervals $(K_1 \text{ and } K_2)$ are mutually independent.

This homogeneous Poisson process of parameter λ is canonically a model for points occurring randomly in time at a uniform of λ per unit interval of time. The intensity measure and intensity function of this are $\Phi([h_1,h_2]) = \lambda(h_2 - h_1)$ and $\lambda(h) = \lambda$ respectively.

The homogeneous Poisson process can be extended to the non-homogeneous Poisson process if the uniform time rate is varied for points that occur randomly in time [29]. This non-homogeneous process also possesses the same independent counts properties but with the adjusted property that for all $K = [h_1, h_2] \subset \mathbb{K}$, the number of points in the interval K follows a Poisson distribution with intensity measure $(\Phi(K))$, i.e. $N(K) \sim \text{Poi}(\Phi(K))$,

where

$$\Phi(K) = \int_{h_1}^{h_2} \lambda(h) dh.$$

The Poisson process has a fundamental property such that the events (points) happen independently of one another. The existence of a point at $x \in K$ location does not influence the existence of other points in a region of x, or elsewhere [29].



2.6.1 The univariate case

The concept of convergence of random variables is required in order to apply point processes representation for extreme values modelling. Assume a series of independent and identically distributed (i.i.d.) random variables with a common distribution function F is represented by X_1, X_2, \ldots, X_n , where $\ddot{M}_n = max\{X_1, \ldots, X_n\}$. The distribution of the normalized maxima, with sequences of constants $\{b_n\}$ and $\{a_n > 0\}$ can be reasonably approximated by a generalized extreme value (GEV) distribution as

$$\Pr\{(\ddot{M}_n - b_n)/a_n \le c\} \rightarrow \ddot{G}(c)$$

with

$$\ddot{G}(c) = \exp\left\{-\left[1 + \xi\left(\frac{c - \mu}{\sigma}\right)\right]^{-\frac{1}{\xi}}\right\},\tag{5}$$

for c_+ and c_- signifying the upper and lower endpoints of \ddot{G} in that order, and ξ , μ and σ (for $\sigma > 0$) are the shape, location and scale parameters respectively. Following this, a sequence of point processes (N_n) is defined as

$$N_n = \{ (i/(n+1), (X_i - b_n)/a_n) \} \text{ for } i = 1, \dots, n.$$
(6)

The first ordinate ensures that the time axis consistently maps to (0,1) while the second ordinate is scaled to sustain stability in the behaviour pattern of extremes as $n \to \infty$ [29].

Now for a sufficiently large value of the threshold u, consider a region of the form $K = [0,1] \times [u,\infty]$ where the point processes sequence N_n converge in distribution to a non-homogeneous Poisson process N for any $u > c_-$, i.e. $N_n \stackrel{d}{\to} N$ as $n \to \infty$. This limit occurs since the random variables X_i are mutually independent and each of the points in \ddot{M}_n has p probability (in equation 7) of falling in the K region, hence $N_n(K)$ follows a binomial distribution, i.e. $N_n(K) \sim \text{Bin}(n, p)$.

$$p = \Pr\left\{\frac{(X_i - b_n)}{a_n} > u\right\} \approx \frac{1}{n} \left[1 + \xi \left(\frac{u - \mu}{\sigma}\right)\right]^{-\frac{1}{\xi}}.$$
 (7)

By the standard approximation of a binomial distribution to a Poisson limit, as $n \to \infty$, the limiting distribution of $N_n(K)$ for any region of the type $K = [h_1, h_2] \times (u, \infty)$, where $[h_1, h_2] \subset [0, 1]$ is the Poisson distribution having intensity measure $\Phi(K)$ i.e. $\operatorname{Poi}(\Phi(K))$ with

$$\Phi(K) = n_{\tilde{y}}(h_1 - h_2) \left[1 + \xi \left(\frac{u - \mu}{\sigma} \right) \right]^{-\frac{1}{\xi}}, \tag{8}$$

where the intensity measure is the average number of points that occur in any given subset $K \subset \mathbb{K}$, $n_{\bar{y}}$ denotes the number of years of observation, and σ , μ , and ξ are the scale, location and shape parameters respectively. Hence, the Poisson process is a realistic approximation of the point processes for large but finite sample behaviour on the specified region where the threshold is sufficiently large [29].

2.7 Formal hypothesis tests for a selected domain of attraction

Any selected domain of attraction, i.e., the Weibull, Gumbel or Fréchet model, for the estimated shape parameter under the GEVD can be tested using formal hypothesis testing procedures such as the likelihood-based methods. The test is necessary especially for practical use because the choice of a wrong model can be terrible (in practice) since it will lead to the choice of erroneous parameters for design. The three models have very different physical meanings due to their tails description. Hence, the need for proper identification of one of the three subfamilies models is very important practically as it is theoretically [37].

2.8 The likelihood-based methods

Based on a given set of data $\mathbf{x} = \{x_1, ..., x_n\}$ with sample size n, these methods will be used to test the hypothesis:

$$H_{\circ}: \xi = 0$$
 (Gumbel)
 $H_{1}: \xi \neq 0$ (Fréchet or Weibull).



Given a parameter vector $\ell(x; \vartheta)$ for the log-likelihood with a function $\vartheta = (\mu, \sigma, \xi)$, where the three parameters represent the location, scale and shape respectively. Let the maximum likelihood estimates of ϑ under H_0 and H_1 be $\hat{\vartheta}_0 = (\hat{\mu}_0, \hat{\sigma}_0, 0)$ and $\hat{\vartheta}_1 = (\hat{\mu}_1, \hat{\sigma}_1, \hat{\xi}_1)$ respectively. These likelihood-based methods can be described under the asymptotically equivalent test of the "likelihood ratio test" [37].

2.9 The likelihood ratio test

The likelihood ratio (LR) test as stated in equation (9) compares $\ell(\mathbf{x}; \hat{\vartheta}_0)$ with $\ell(\mathbf{x}; \hat{\vartheta}_1)$. That is, it compares the evaluation of the likelihood at $\hat{\vartheta}_0$ with the evaluation of the likelihood at $\hat{\vartheta}_1$.

$$LR = 2\{\ell(\mathbf{x}; \hat{\vartheta}_1) - \ell(\mathbf{x}; \hat{\vartheta}_0)\},\tag{9}$$

where LR is a χ^2 with 1 degree of freedom under the null hypothesis H_{\circ} .

For a better accuracy to the approximation of asymptotic distribution of the likelihood ratio test *LR*, a modification suggested by Hosking [38] is given as

$$LR_{**} = \left(1 - \frac{2.8}{w}\right)LR,\tag{10}$$

where w is the sample values i.e. the number of exceedances or cluster-maxima above the threshold u. A decision for the rejection of H_0 can be made at a level of significance α if

$$LR_{**} > \chi_1^2 (1 - \alpha).$$
 (11)

The critical values $\chi_1^2(1-\alpha)$ is the $(1-\alpha)$ quantile of the χ^2 distribution with 1 degree of freedom [37].

3 Results and discussions

3.1 Data description

The raw price data used for this study include the daily closing equity indices of the Brazilian, Russian, Indian, Chinese and South African stock markets. The data were obtained from Thomson Reuters Datastream and are for the period 5th January 2010 to 6th August 2018 with 2126 observations. The Brazilian market index is called the "Bovespa index", abbreviated - IBOV; the Russian market index is called the "Moscow Exchange index", abbreviated - IMOEX; the Indian market index is called the "NIFTY 50 index", abbreviated - NIFTY; the Chinese market index is called the "Shanghai Stock Exchange Composite", abbreviated - SHCOMP; and lastly, the South African market index is called the "JSE Africa All Share index", abbreviated - JALSH.

3.2 Missing values

It was observed for the period under study that seven daily closing indices values were missing in the markets. These were adjusted using simple imputation methods in "mice" package developed by Buuren and Groothuis-Oudshoorn [39] in *R* application software. The cleaned data were averaged in the affected markets to produce average daily closing values.

3.3 Volatility filtration

Before applying the univariate EVT models of the CEV (via GPD fit) and point process for modelling the risk, volatility needs to be filtered out since it is known that the removal of short-range linear dependence and ARCH effects or heteroscedasticity from the financial returns makes the EVT modelling more satisfactory [20]. Several candidate ARMA(p,q)-GARCH(k,v) models were run to obtain a combined model that can best remove linear dependency and heteroscedasticity in the return series. From the candidate models, ARMA(1, 1) and GARCH(1, 1) are jointly and parsimoniously selected as the most adequate for the Brazilian, Russian, Indian, Chinese and South African equity markets.



783 H 1	 •	4 T	CIT	T	3 4	
- Iah		ΔR	CH		1/1	test.

	Brazil	Russia	India	China	S/Africa
	(Bovespa)	(IMOEX)	(NIFTY)	(SHCOMP)	(JALSH)
ARCH LM test (5)	74.69051	146.3231	136.7945	275.4920	126.4324
<i>p</i> -value (5)	(0.0000)	(0.0000)	(0.0000)	(0.0000)	(0.0000)
With $GARCH(1, 1)$:					
ARCH LM test (5)	0.3741	0.1038	0.4484	1.4610	0.9945
<i>p</i> -value (5)	(0.9200)	(0.9861)	(0.8987)	(0.6026)	(0.7346)

ARCH LM test (5) denotes ARCH effects up to the 5^{th} order with p-values in brackets at 5% level of significance.

The fitting of this joint ARMA(1, 1)-GARCH(1, 1) model is carried out under seven error distributions of a normal, skewed-normal, Student's t, skewed-Student's t, generalized error distribution (GED), skewed-GED and the generalized hyperbolic distribution (GHYP). ARCH LM test is used to test for the presence of ARCH effects before and after fitting the GARCH(1, 1) model on the residuals of the return series. As for the outcomes, similar results were obtained for the fit under all the seven error distributions. However, due to space constraint, only the results under the Student's t are shown as displayed in Table 1. From the table, before fitting GARCH(1, 1) model, the p-values under each of the five markets are highly significant at 1%, indicating the presence of ARCH effects, but after fitting GARCH(1, 1) model on the residuals, the ARCH effects were filtered out as shown by the outcomes of the p-values that are all greater than 0.05.

3.4 Risk modelling

The risk in each of the five BRICS equity markets is modelled using the univariate versions of the two models: the CEV and point process.

3.5 The conditional univariate extreme value (CUEV) model

This is the univariate version of the CEV model that fits the GPD to marginal variables. Hence, the GPD will be fitted to each of the BRICS return's residuals to obtain the magnitude of the risks in the markets. For consistency and comparison, the same steps are followed in the modelling and analysis of risk in each of the markets. These steps include: threshold selection and diagnostics, sensitivity analysis for a suitable threshold choice, declustering of threshold exceedances, parameters' estimation and diagnostics, return levels analysis and diagnostics.

3.6 Large positive and negative residual observations

From the GARCH regression equation of the financial return r_t stated as

$$r_t = \mu + \varepsilon_t. \tag{12}$$

The residual ε_t becomes,

$$\varepsilon_t = r_t - \mu_t,\tag{13}$$

$$\varepsilon_t = r_t - \hat{r}_t,\tag{14}$$

where r_t and \hat{r}_t are the return observations (observed values) and the predicted or estimated values respectively. If

$$\varepsilon_t > 0$$
, then $r_t > \hat{r}_t$, otherwise it is, (15)

$$\varepsilon_t < 0 \Rightarrow r_t < \hat{r}_t. \tag{16}$$

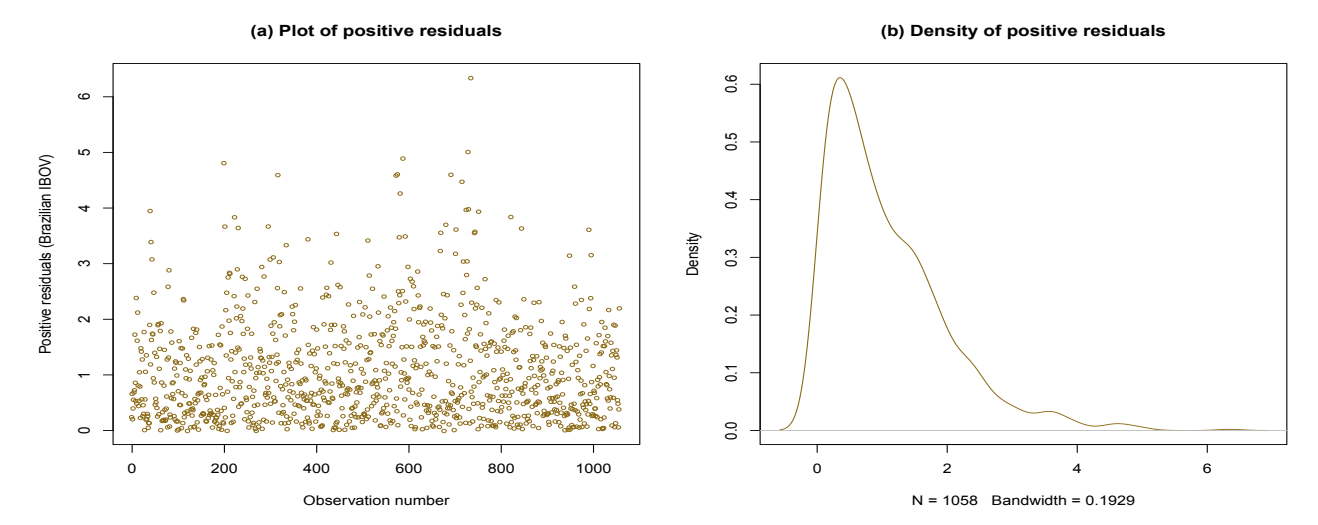


Fig. 1: IBOV: Positive residuals.

Equation (15) implies that when the observed return value r_t is greater than the estimated or predicted value \hat{r}_t , the residual is positive $\varepsilon_t > 0$ and that amounts to under-prediction, which corresponds to financial losses. Otherwise, it is over-prediction with a negative residual $\varepsilon_t < 0$ and it relates to gains (equation 16). That is, large or extreme positive and negative residuals relate to losses and gains respectively [14]. This study is primarily interested in modelling the unexplained large positive residuals which reflect extreme financial losses in the BRICS return series.

3.7 Positive residual observations

The modelling of the risk in each of the markets is restricted to the positive residuals of the entire equity observations. From the original equity data with 2126 number of observations, there are 1058, 1034, 1073, 1113 and 1095 positive residual observations in the Brazilian IBOV, Russian IMOEX, Indian NIFTY, Chinese SHCOMP and South African JALSH markets respectively. Figure 1, panels (a) and (b), shows the visual of the positive residual observations and their corresponding density for the Brazilian IBOV market. The visual plots of the other four markets are not displayed because of space.

3.8 Threshold selection

Two threshold selection models are used in the BRICS markets for the selection of an appropriate threshold. The first model is the "extreme value mixture models" and the second is the "shape threshold stability plot". The latter model is used to verify the outcome of the former model.

The extreme value mixture models can be implemented under the parametric, semi-parametric and non-parametric approaches. This study used the non-parametric approach over the other two approaches because it provides the best tail estimator if the population distribution (of the market's return) is unknown [34], and furthermore, it is more robust to bulk model than the parametric technique [40]. In the non-parametric mixture model, we have the bulk model where a kernel density is fitted and a GPD is fitted to the tail. The resulting mixture model is then called the Kernel-GPD (KenGPD) model. That is, the bulk model under the threshold is the standard kernel density estimator and the tail model is a GPD above the threshold. The threshold can be estimated using either the bulk model based or the parameterized tail fraction approach.

Following the threshold selection steps of Hu and Scarrott [34], this study combined the plots of the bulk model based tail fraction and the parameterized tail fraction approaches on the same diagram and used their diagnostic plots to assess which of the two gives a better threshold's parameter estimate (see Figure 2 for the Brazilian IBOV market). The figure shows the output of the bulk model based tail fraction (blue solid line), where the threshold value u = 2.1731. For the parameterized tail fraction (red solid line) approach, u = 2.1725 is obtained. These threshold values are approximately the same, hence they overlapped, where the red colour of the density and threshold line of the parameterized tail fraction almost completely overshadows the blue colour of that of the bulk model based tail fraction.





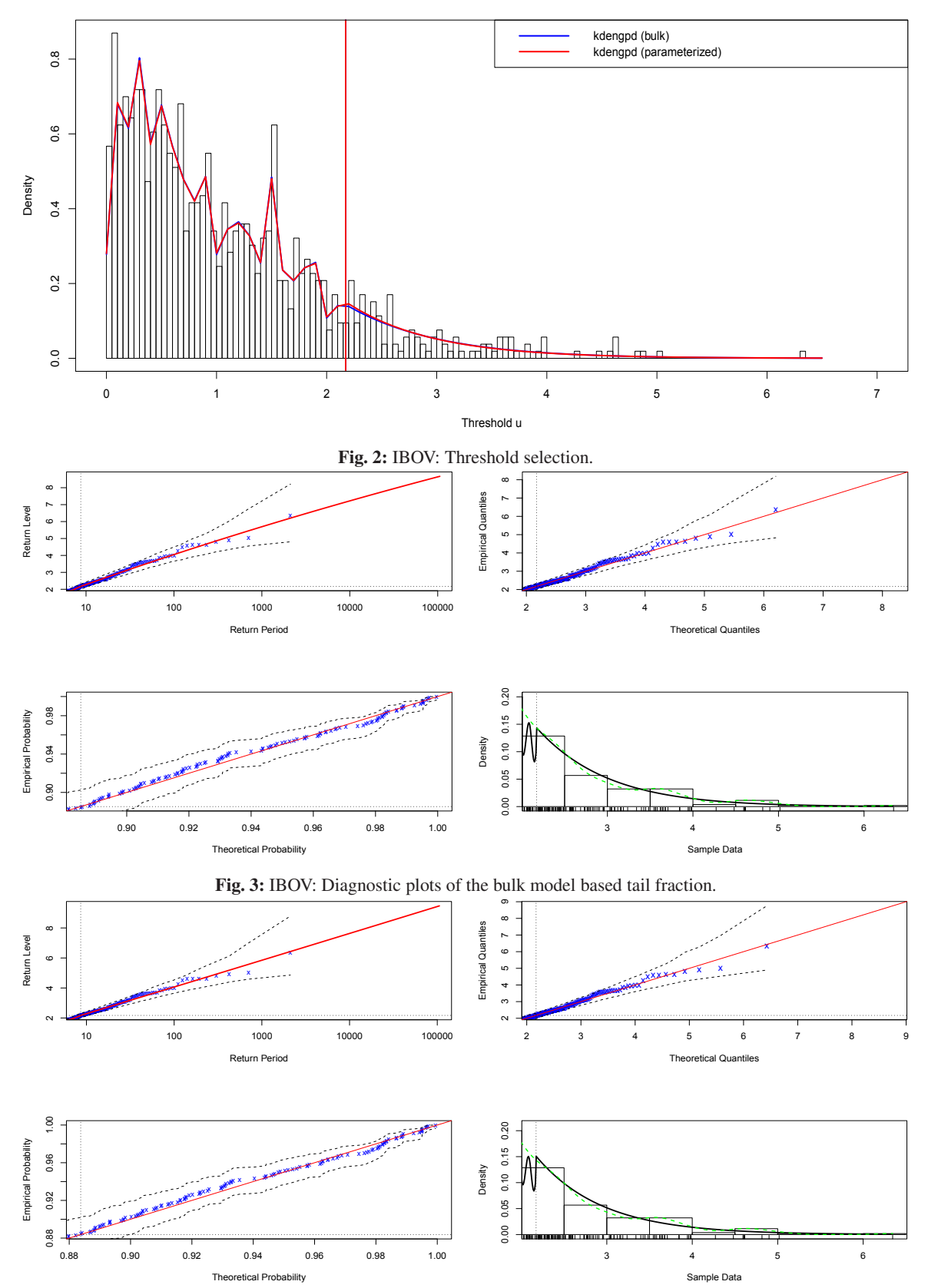


Fig. 4: IBOV: Diagnostic plots of the parameterized tail fraction.



For the Russian IMOEX market, the combined plots of the bulk model based (blue solid line) and the parameterized tail fraction (red solid line) approaches are displayed in Figure 12 in the Appendix. The figure shows the output of the bulk model based tail fraction with threshold u = 2.6890, and that of the parameterized tail fraction approach at u = 3.0847. Because of space, only the threshold outcomes of the three remaining markets (i.e., NIFTY, SHCOMP and JALSH) are presented, their plots are not displayed. For the Indian NIFTY market, threshold values u = 1.9694 and u = 1.9689 are obtained for the bulk model based and the parameterized tail fraction approaches respectively. For the Chinese SHCOMP market, a threshold value u = 2.2112 is obtained for the parameterized tail fraction approach, and u = 1.8178 for the bulk model based tail fraction. Lastly for the South African JALSH market, on the combined plots, the parameterized tail fraction approach produced a threshold value u = 2.2112, and the bulk model based tail fraction gave u = 1.8178.

3.9 Diagnostic plots of the bulk and parameterized approaches

For the Brazilian IBOV market (in Figures 3 and 4) and the Indian NIFTY market (not displayed), there is no obvious difference between the diagnostic plots of the two tail fraction approaches since the threshold values are roughly the same. But, from a closer scrutiny, the diagnostic plots of the fitted parameterized tail fraction show a slightly higher levels of accuracy in linearity of the data points when compared to that of the bulk model based. The data points are more closely aligned on the straight lines of the "return level", "quantiles", and "probability" plots than they are observed in the bulk model based approach for the Brazilian market, and closer alignment of the data points on the straight lines especially on the probability plot of the Indian market. This therefore gives the parameterized tail fraction a bit of an edge over the bulk model based for the threshold selection in these markets.

For the Russian IMOEX market (in Figures 13 and 14), and the Chinese SHCOMP market (not displayed), the various diagnostic plots for assessing the goodness of each of the tail fraction approaches are shown. There is an improvement in the plots of the parameterized tail fraction when compared to that of the bulk model based. The data points are more closely aligned on the diagonal lines of the return level, quantiles and probability plots than they are in the bulk model based approach. Also for the South African JALSH market (not displayed), despite the seeming similarities in the plots of the parameterized and bulk tail fractions, density estimate seems more consistent with the histogram of the data for the diagnostic plot of the parameterized tail fraction than it is for the bulk model based.

The parameterized tail fraction approach makes provision for an extra degree of freedom that is used to re-scale both the bulk and tail components [34]. This enhances and improves the tail fit, since the tail fraction is estimated from the sample fraction of exceedances. Hence, a better fit below an estimated threshold is allowed by the mixture because of this re-scaling of the bulk density. This is not the case with the bulk model based tail fraction because it does not adjust the density below the threshold [34]. Hu and Scarrott [34] also indicated that the bulk model based tail fraction exposes estimation of the tail to the misspecification of the bulk model. This is a major shortcoming to the use of the bulk model based which the parameterized tail fraction approach corrects by using an extra parameter for the tail fraction. For this reason, the parameterized tail fraction approach reduces the effect of the bulk model's misspecification on the tail estimates.

However, the diagnostic plots of the two tail fraction methods summarily suggest that the fit of the non-parametric Kernel-GPD models is satisfactory based on the consistency of the density estimate with the histogram of the data, and the linearity of the data points in the return level, quantiles and probability plots.

3.10 Extremal index for final threshold choice

Following Ferro [33] and Ferro and Seger [41], a sensible choice of an appropriate threshold is where the extremal index (θ) is greater than or equal to 0.5, hence a minimum of $\theta=0.5$ is used in this study for final threshold selection, required for declustering of the cluster exceedances. In order to determine this appropriate threshold, it is required that the plot of "normalised inter-exceedance times" against "standard exponential quantiles" should be piecewise-linear with a breakpoint at the $(1-\theta)$ -quantile, $-\log\theta$ (see Figure 5 and Ferro [33] for details). The sloping line has gradient θ^{-1} , and the vertical line is indicated by the $(1-\theta)$ -quantile. Based on this, a sensitivity analysis will be carried out under each market to ascertain the plot of a suitable threshold that will be best piecewise-linear with extremal index θ of (a minimum of) 0.5.

3.11 Sensitivity analysis

In order to obtain a suitable threshold value where the exceedances are piecewise-linear with a minimum extremal index of 0.50, a sensitivity analysis was carried out as displayed in Figure 5 for the Brazilian market. The sensitivity analysis



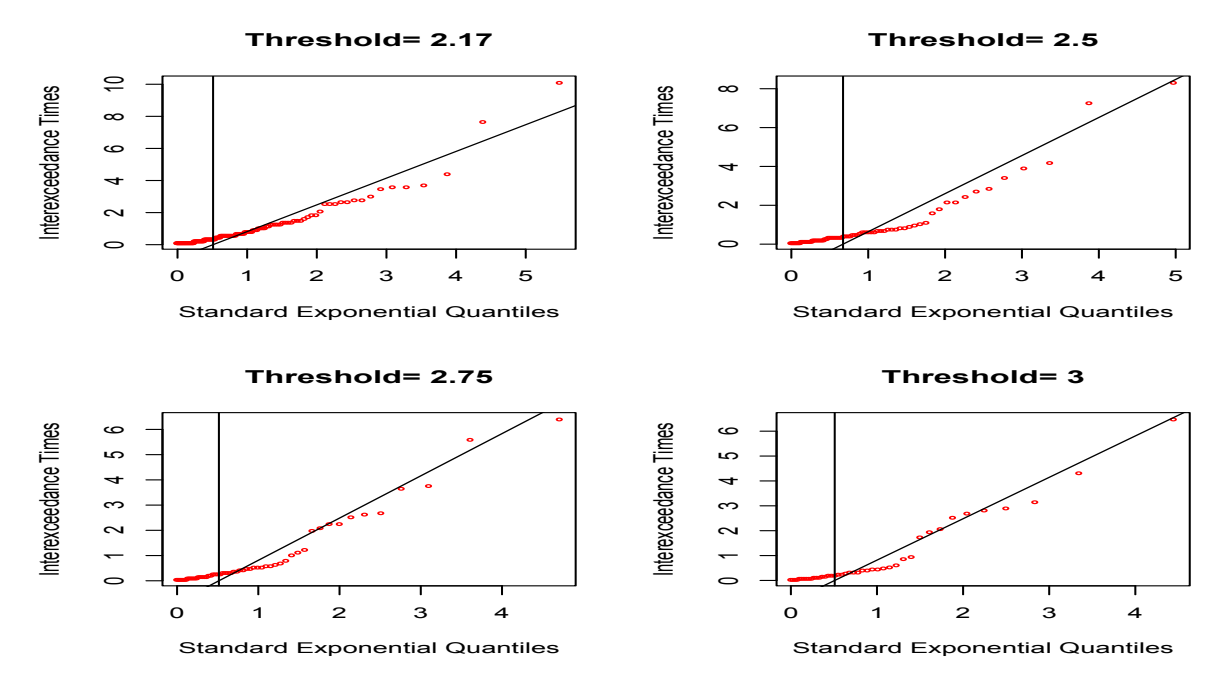


Fig. 5: IBOV: Sensitivity analysis plots for threshold selection.

is initiated with the approximate threshold value of u=2.17 obtained from the parameterized tail fraction approach since its diagnostic plots display slightly higher levels of linearity than the bulk tail fraction approach. Out of the four sensitivity plots with different thresholds in the figure, threshold u=2.17 is chosen because it is the most appropriate on the sensitivity analysis plot in terms of piecewise-linearity with extremal index $\hat{\theta}$ of 0.6002. This means that exceedances occur in groups of $\frac{1}{0.6002} = 1.666 \approx 2$. In this section, we only displayed the sensitivity analysis plots of the Brazilian market and none of the plots of the remaining four markets due to space.

For the Russian market, because the diagnostic plots of the parameterized tail fraction approach show more levels of linearity than the bulk model based, a sensitivity analysis is done starting with its threshold value u = 3.09. From the figure, a piecewise-linearity of the data points are most observed at the plot with threshold u = 3.09 than at the other plots. This threshold gives more asymptotic information about the tail (than the other thresholds) with 80 threshold exceedances and extremal index $\hat{\theta}$ of 0.5521. This means that exceedances occur in groups of $\frac{1}{0.5521} = 1.8113 \approx 2$. For the Indian market, from the set of sensitivity analysis plots, threshold u = 2.25 is chosen because it is the best in the set, and it gives more tail information (than the other three plots) with 70 threshold exceedances and extremal index $\hat{\theta} = 0.5852$. An extremal index of 0.5852 means that exceedances occur in groups of $\frac{1}{0.5852} = 1.7088 \approx 2$.

For the Chinese equity market, the estimated threshold value u = 1.9751 from the parameterized tail fraction approach is used as the starting point for the sensitivity analysis due to its superior diagnostics accuracy. However, the extremal index $\hat{\theta}$ at this threshold value is lower than 0.5, hence it is not chosen. It is observed in this sensitivity analysis that extremal index $\hat{\theta}$ is greater than 0.5 from threshold value u = 2.86 and above. At threshold u = 2.86, the extremal index is 0.5349 with 43 threshold exceedances, hence exceedances occur in groups of $\frac{1}{0.5349} = 1.8695 \approx 2$. This threshold estimate gives more information about the tail with more exceedance observations than the other remaining two thresholds. Based on this, threshold estimate u = 2.86 is chosen. Lastly, for the South African market, the threshold value u = 2.21 obtained from the parameterized tail fraction approach is used as an initial value for the sensitivity analysis. From the plots, threshold value u = 2.60 is chosen because it displays the best piecewise linearity of points with extremal index $\hat{\theta} = 0.5117$ than the rest of the plots. This means that exceedances occur in groups of $\frac{1}{0.5117} = 1.9543 \approx 2$.

3.12 Shape threshold stability plot

The traditional shape threshold stability plot is used in this study to verify and give some levels of credence to the threshold choice from the Kernel density mixture models. As displayed in Figure 6 for the Brazilian market, three potential thresholds where the plot shows significant departures from linearity are identified around u = 1.0, u = 1.5 and u = 2.2.



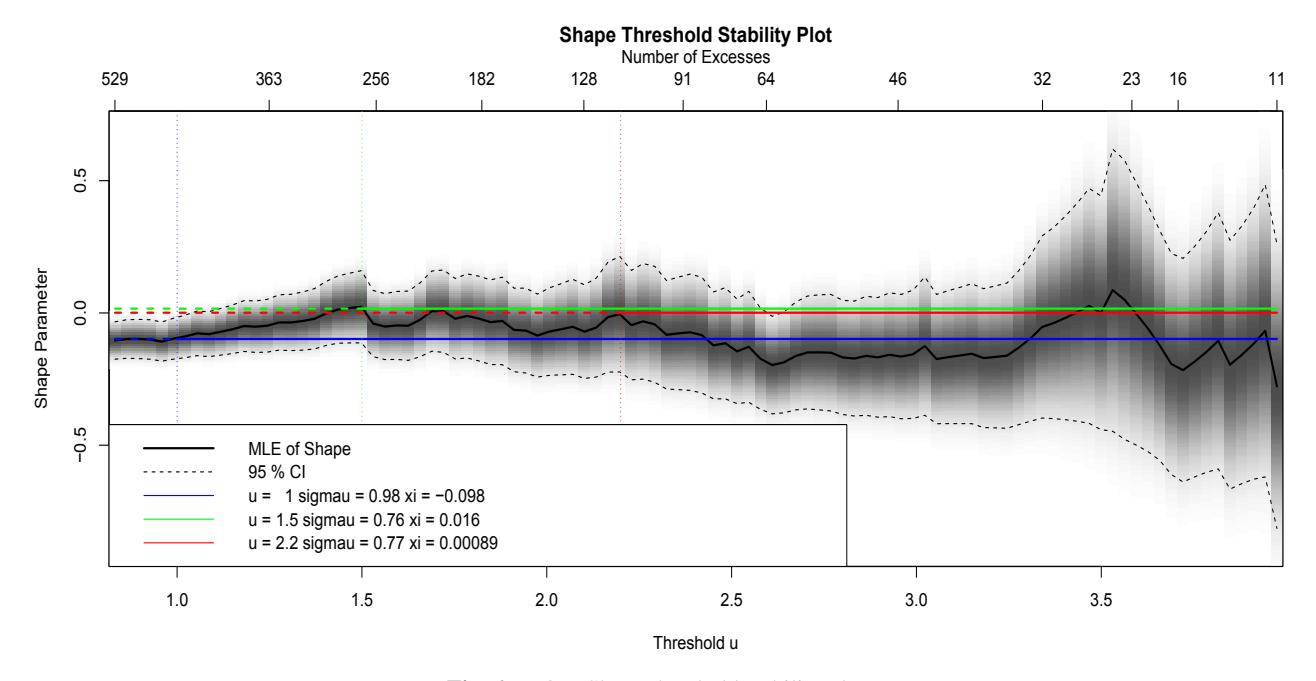


Fig. 6: IBOV: Shape threshold stability plot.

Therefore, it can be seen that the choice of u = 2.2 from the shape threshold stability plot is approximately consistent with the threshold estimate (u = 2.17) from the Kernel density mixture models.

The plots of the remaining four equity markets are not displayed but the outcomes are presented. For the Russian equity market, the three potential thresholds where the plot shows significant departures from linearity are identified around u =1.5, u = 2 and u = 3. Hence, the threshold estimate (u = 3.09) from the Kernel density mixture models is approximately consistent with the choice of u = 3 from the shape threshold stability plot. For the Indian market, from the shape threshold stability plot, the three potential thresholds identified for significant departures from linearity are u = 1.2, u = 1.9 and u =2.2. One of these subjective choice of thresholds, i.e. u = 2.2 is approximately consistent with the threshold estimate u = 2.22.25 from the Kernel density mixture models. Hence, the objective threshold choice of the Kernel-GPD is a fair tradeoff between variance and bias.

For the Chinese market, significant departures from linearity can be seen at u = 1.3, u = 1.9 and u = 2.4. The threshold estimate u = 2.4 is not far from the threshold u = 2.86 obtained by the parameterized tail fraction of the Kernel density mixture models. From the shape threshold stability plot in the South African market, thresholds u = 2.5, u = 2.7 and u =3.1 are identified for significant departures from linearity. The threshold choices u = 2.5 and u = 2.7 are close to and are approximately consistent with the threshold estimate of u = 2.60 from the Kernel density mixture models.

3.13 Declustering

The process of modelling extreme observations using a threshold exceedance model generally faces the problems of dependence that usually exists because of short-term clustering of exceedances [29]. The EVT approach fits a Poisson process using the point process model and the GPD (via the CEV model) to "independent" excesses (or exceedances) above some appropriately high threshold. It is empirically believed that threshold excesses do not essentially exist separately, but are clustered together most of the time [42]. Hence, to ensure that the exceedances are independent, the time series undergoes the process of declustering, where the dependent observations are filtered to obtain a set of threshold exceedances that are approximately independent [29,43].

For the Brazilian market, 123 threshold exceedances are generated at the estimated threshold u = 2.17. After declustering at this threshold, 71 cluster-maxima are obtained as shown in Figure 7. The declustered exceedances plots of the four remaining markets are not displayed. For the Russian IMOEX market, the estimated threshold u = 3.09generated 80 threshold exceedances. After declustering at the threshold, 45 cluster-maxima are obtained. For Indian NIFTY market, the estimated threshold u = 2.25 generated 70 threshold exceedances, and produced 39 cluster-maxima after declustering at this threshold. For the Chinese SHCOMP market, the threshold estimate u = 2.86 generated 43

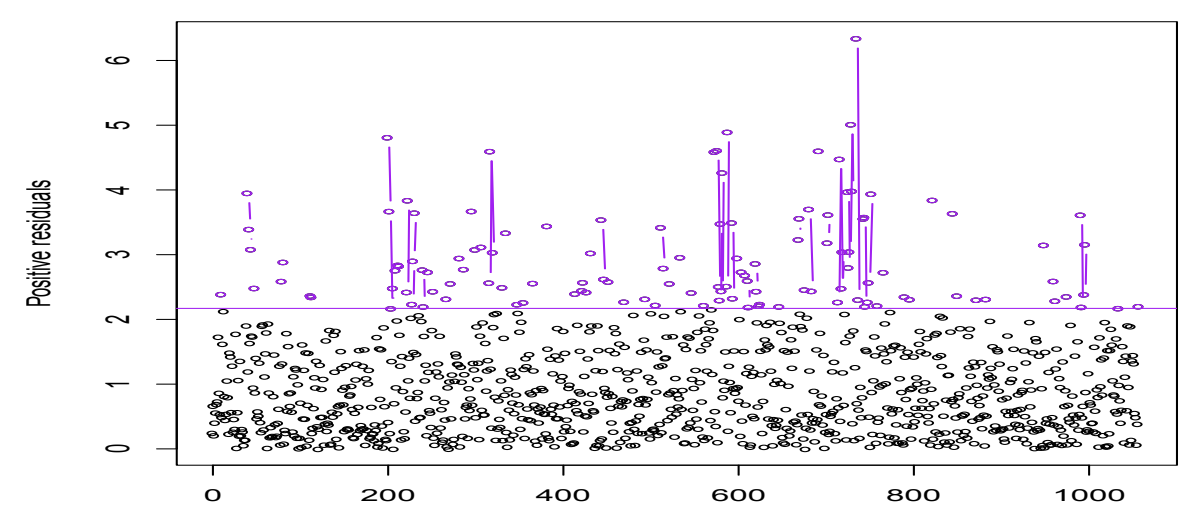


Fig. 7: IBOV: Declustered exceedances at u = 2.17 (cluster-maxima).

threshold exceedances which were declustered and 23 cluster-maxima are obtained. For the South African JALSH market, the estimated threshold u = 2.60 generated 76 threshold exceedances. After declustering at this threshold, 36 cluster-maxima are obtained. The cluster-maxima are the maxima of the clusters of exceedances over a high threshold. They are the independent extreme tail observations on which the GPD will be fitted, and are also called exceedance residuals [14].

3.14 CEV model: GPD fit to cluster-maxima

Since the univariate version of the CEV model fits the GPD to marginal variables, the GPD will now be fitted to the cluster-maxima that are generated after declustering the cluster exceendances. These cluster-maxima are collectively classified as the risks, which are the extreme financial losses, to be modelled in the markets. The risks are modelled by fitting the GPD to the 71, 45, 39, 23, 36 cluster-maxima observations in the Brazilian IBOV, Russian IMOEX, Indian NIFTY, Chinese SHCOMP and South African JALSH markets respectively, and the results in Table 2 are obtained, where the standard errors of the GPD estimates are enclosed in parentheses and the confidence intervals are in the brackets. For the confidence intervals estimation, the delta method or profile likelihood intervals approach can be used. However, the application of profile likelihood intervals approach gives better interval accuracy than does the delta method [29]. Hence, only the estimated results of the profile likelihood intervals approach are presented in the table. The profile confidence intervals in this study are computed using the "POT" package developed by Ribatet [44] in R statistical software. The table also includes the sample proportion η_u of points, which are the cluster-maxima exceeding the thresholds. This sample proportion is the ratio of the number of cluster-maxima w to the total positive residual observations n.

For the Russian IMOEX market, the positive estimate ($\xi=0.14$) of the shape parameter as shown in the table denotes a heavy or fat-tailed distribution and it is a reflection of concavity [29]. The shape parameter estimates for the Brazilian IBOV, Indian NIFTY, Chinese SHCOMP and South African JALSH markets are $\xi=-0.05$, $\xi=-0.17$, $\xi=-0.25$, and $\xi=-0.05$ respectively (see Table 2). These shape parameters' negative estimates indicate a short tailed distribution that reflects convexity [](Coles, 2001). However, since the values of the confidence intervals of the estimated shape parameters at the three confidence levels in the table are all from negative to positive, i.e. they include zero, a formal hypothesis test is carried out in Section 3.15 using the likelihood ratio (LR) and the modified likelihood ratio (LR_{**}) tests (as described in Sections 2.7 to 2.9) to determine if $\xi=0$ or otherwise.

3.15 Formal hypothesis test

The likelihood ratio (LR) and modified likelihood ratio (LR_{**}) tests are used with the null hypothesis that $\xi = 0$ against the alternative hypothesis that $\xi \neq 0$. From the outcome in Table 3, at the 1%, 5% and 10% levels of significance, the values of the likelihood ratio (LR) and the modified likelihood ratio (LR_{**}) tests are less than the critical values (CV), therefore we fail to reject the null hypothesis, implying that the shape parameter $\xi = 0$. This suggests a Gumbel domain



Table 2: GPD parameter estimates and profile likelihood intervals.

Indices	CI	и	n	w	$\eta_u = \frac{w}{n}$	ξ	σ̂	Log. lik
	90%	2.17	1058	71	0.0671	-0.05 (0.14)	0.94 (0.18)	-62.57
Brazil						[-0.22; 0.23]	[0.68; 1.24]	
IBOV	95%	2.17	1058	71	0.0671	-0.05 (0.14)	0.94 (0.18)	-62.57
						[-0.22; 0.30]	[0.64; 1.31]	
	99%	2.17	1058	71	0.0671	-0.05 (0.14)	0.94 (0.18)	-62.57
						[-0.22; 0.45]	[0.56; 1.44]	
	90%	3.09	1034	45	0.0435	0.14 (0.16)	1.25 (0.22)	-61.63
Russian						[-0.05; 0.50]	[0.86; 1.77]	
IMOEX	95%	3.09	1034	45	0.0435	0.14 (0.16)	1.25 (0.22)	-61.63
						[-0.08; 0.59]	[0.79; 1.89]	
	99%	3.09	1034	45	0.0435	0.14 (0.16)	1.25 (0.22)	-61.63
						[-0.11; 0.78]	[0.68; 2.14]	
	90%	2.25	1073	39	0.0364	-0.17 (0.16)	1.14 (0.22)	-37.36
Indian						[-0.30; 0.16]	[0.77; 1.63]	
NIFTY	95%	2.25	1073	39	0.0364	-0.17 (0.16)	1.14 (0.22)	-37.36
						[-0.30; 0.24]	[0.72; 1.74]	
	99%	2.25	1073	39	0.0364	-0.17 (0.16)	1.14 (0.22)	-37.36
						[-0.30; 0.41]	[0.64; 1.98]	
	90%	2.86	1113	23	0.0207	-0.25 (0.18)	0.98 (0.27)	-16.75
Chinese						[-0.36; 0.16]	[0.66; 1.53]	
SHCOMP	95%	2.86	1113	23	0.0207	-0.25 (0.18)	0.98 (0.27)	-16.75
						[-0.36; 0.27]	[0.67; 1.68]	
	99%	2.86	1113	23	0.0207	-0.25 (0.18)	0.98 (0.27)	-16.75
						[-0.36; 0.53]	[0.67; 2.01]	
	90%	2.60	1095	36	0.0329	-0.05 (0.20)	1.16 (0.26)	-39.51
S/African						[-0.29; 0.35]	[0.75; 1.77]	
JALSH	95%	2.60	1095	36	0.0329	-0.05 (0.20)	1.16 (0.26)	-39.51
						[-0.29; 0.44]	[0.68; 1.93]	
	99%	2.60	1095	36	0.0329	-0.05 (0.20)	1.16 (0.26)	-39.51
						[-0.29; 0.67]	[0.57; 2.27]	

Table 3: Likelihood ratio test for GPD's ξ estimate.

	w	ξ̂	LR	CV	LR_{**}	CV
Brazilian IBOV	71	-0.05	-125.14	10%: 2.706	-120.21	10%: 2.706
				5%: 3.841		5%: 3.841
				1%: 6.635		1%: 6.635
Russian IMOEX	45	0.14	-123.26	10%: 2.706	-115.59	10%: 2.706
				5%: 3.841		5%: 3.841
				1%: 6.635		1%: 6.635
Indian NIFTY	39	-0.17	-74.72	10%: 2.706	-69.36	10%: 2.706
				5%: 3.841		5%: 3.841
				1%: 6.635		1%: 6.635
Chinese SHCOMP	23	-0.25	-33.50	10%: 2.706	-29.42	10%: 2.706
				5%: 3.841		5%: 3.841
				1%: 6.635		1%: 6.635
S/African JALSH	36	-0.05	-79.02	10%: 2.706	-72.87	10%: 2.706
				5%: 3.841		5%: 3.841
				1%: 6.635		1%: 6.635

w is the number of cluster-maxima observations and CV is the critical value.



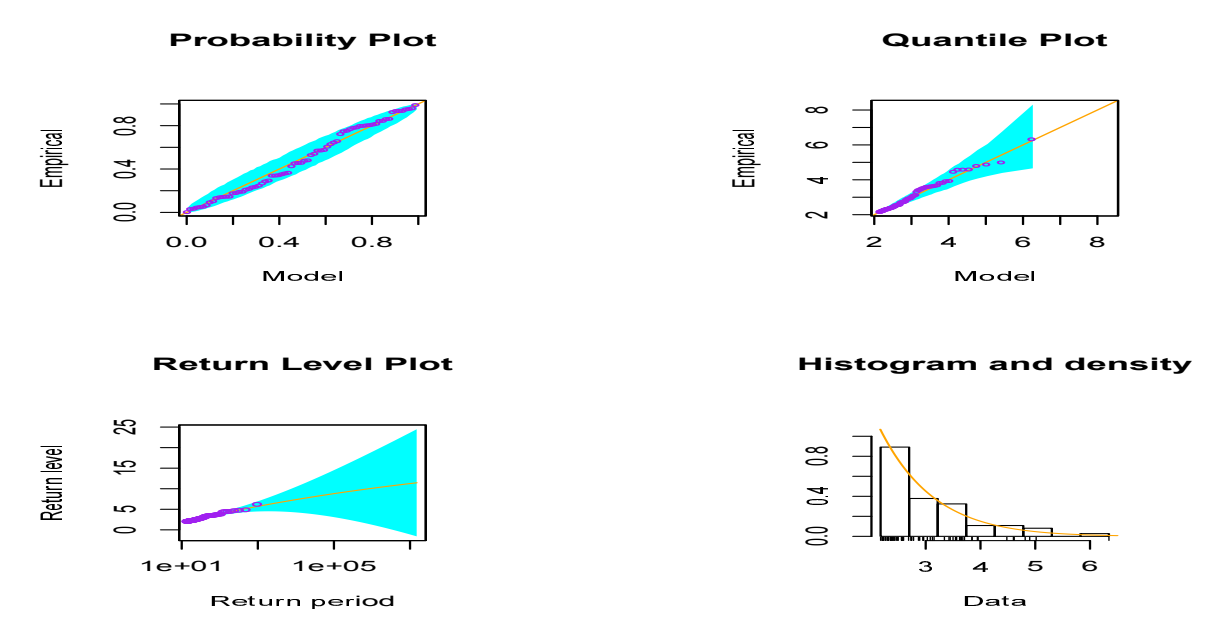


Fig. 8: IBOV: GPD diagnostic plots.

of attraction for the data, hence the risks in the Brazilian IBOV, Russian IMOEX, Indian NIFTY, Chinese SHCOMP and South African JALSH markets using the CEV's GPD fit can be modelled by the Gumbel class of distributions.

3.16 Diagnostics: Model checking

Statistical models are fit to data so as to make reasonable conclusions about the population where the data is drawn. Model diagnostics are used to ascertain the validity of a model. The accuracy of a model can be checked or judged using diagnostics to know whether it agrees with the data used to estimate it.

Four diagnostic plots are displayed in Figure 8 and in each of Figures 15, 16, 17 and 18 in the Appendix to assess the performance of the GPD fit to the 71, 45, 39, 23, 36 cluster-maxima in the Brazilian IBOV, Russian IMOEX, Indian NIFTY, Chinese SHCOMP and South African JALSH markets respectively. For each quartet plots, the data points in the quantile plot, probability plot and return level plot are near-linear, and the corresponding density estimate appears consistent with the histogram of the cluster-maxima. None of these four plots in each market gives any real cause for concern about the quality of the fitted GPD model. Consequently, the diagnostic plots give support to the validity of the GPD fit.

3.17 Goodness of fit of the GPD

The goodness of fit tests of Anderson-Darling and Cramér-von Mises are further used to ascertain how well the GPD model fits the cluster-maxima observations in the IBOV, IMOEX, NIFTY, SHCOMP and JALSH market indices. The tested hypothesis are:

 H_{\circ} : GPD fits the cluster-maxima well

 H_1 : GPD does not fit the cluster-maxima well

Table 4 displays the outcomes of the test statistics and *p*-values of the tested hypothesis of the Anderson-Darling and Cramér-von Mises tests. For both goodness of fit tests, it is observed that the null hypothesis is not rejected since each test's *p*-value is large (greater than 0.05) in the five BRICS markets. This indicates that the GPD fits the generated cluster-maxima observations well.



 Table 4: Goodness of fit test.

	Test	GPD values	Statistic values	P-value
	Anderson-Darling	σ: 0.94	0.4209	0.4788
IBOV		ξ: -0.05		
	Cramér-von Mises	σ: 0.94	0.0559	0.5126
		ξ: -0.05		
	Anderson-Darling	σ: 1.25	0.3384	0.6136
IMOEX		ξ: 0.14		
	Cramér-von Mises	σ: 1.25	0.0420	0.6673
		ξ: 0.14		
	Anderson-Darling	σ: 1.14	0.3767	0.5964
NIFTY		ξ: -0.17		
	Cramér-von Mises	σ: 1.14	0.0498	0.6260
		ξ: -0.17		
	Anderson-Darling	σ: 0.98	0.3958	0.5767
SHCOMP		ξ: -0.25		
	Cramér-von Mises	σ: 0.98	0.0537	0.5950
		ξ: -0.25		
	Anderson-Darling	σ: 1.16	0.3565	0.6110
JALSH		ξ: -0.05		
	Cramér-von Mises	σ: 1.16	0.0458	0.6512
		ξ: -0.05		

Table 5: GPD return level (\ddot{R}_g) estimates.

IBOV	2-year	5-year	10-year	20-year	50-year
$\widehat{\ddot{R}_g}$	7.41	8.00	8.44	8.86	9.39
90% <i>CI</i>	(4.73; 10.09)	(4.51; 11.50)	(4.27; 12.61)	(3.97; 13.75)	(3.49; 15.29)
95% CI	(4.21; 10.60)	(3.84; 12.17)	(3.47; 13.41)	(3.03; 14.68)	(2.36; 16.42)
99% CI	(3.21; 11.60)	(2.53; 13.48)	(1.91; 14.97)	(1.21; 16.51)	(0.16; 18.63)
IMOEX	2-year	5-year	10-year	20-year	50-year
$\widehat{\ddot{R}_{g}}$	16.87	20.03	22.72	25.69	30.10
90% <i>CI</i>	(5.58; 28.15)	(3.60; 36.47)	(1.36; 44.09)	(-1.66; 53.05)	(-7.07; 67.28)
95% CI	(3.42; 30.32)	(0.45; 39.61)	(-2.74; 48.18)	(-6.90; 58.29)	(-14.19; 74.40)
99% CI	(-0.80; 34.54)	(-5.69; 45.76)	(-10.72; 56.17)	(-17.13; 68.51)	(-28.09; 88.29)
NIFTY	2-year	5-year	10-year	20-year	50-year
$\widehat{\ddot{R}_g}$	6.76	7.08	7.29	7.47	7.69
90% CI	(4.71; 8.81)	(4.57; 9.59)	(4.43; 10.14)	(4.27; 10.67)	(4.04; 11.33)
95% CI	(4.32; 9.20)	(4.09; 10.07)	(3.88; 10.69)	(3.66; 11.28)	(3.35; 12.02)
99% CI	(3.56; 9.97)	(3.15; 11.00)	(2.81; 11.76)	(2.46; 12.48)	(1.99; 13.39)
SHCOMP	2-year	5-year	10-year	20-year	50-year
$\widehat{\ddot{R}_g}$	6.03	6.19	6.29	6.37	6.46
90% CI	(4.75; 7.31)	(4.68; 7.70)	(4.61; 7.96)	(4.54; 8.20)	(4.43; 8.48)
95% CI	(4.37; 7.69)	(4.23; 8.15)	(4.11; 8.46)	(3.99; 8.75)	(3.83; 9.08)
99% CI	(3.61; 8.46)	(3.32; 9.06)	(3.10; 9.47)	(2.89; 9.85)	(2.62; 10.29)
JALSH	2-year	5-year	10-year	20-year	50-year
$\widehat{\ddot{R}_g}$	9.12	9.86	10.41	10.93	11.60
90% <i>CI</i>	(4.43; 13.80)	(3.75; 15.98)	(3.11; 17.70)	(2.38; 19.49)	(1.27; 21.93)
95% CI	(3.53; 14.70)	(2.58; 17.15)	(1.72; 19.10)	(0.74; 21.12)	(-0.71; 23.91)
99% CI	(1.78; 16.45)	(0.29; 19.43)	(-1.01; 21.83)	(-2.46; 24.32)	(-4.57; 27.77)

-0.05 (0.14) [-0.28; 0.17] -0.05 (0.14) [-0.32; 0.22] -0.05 (0.14) [-0.40; 0.30] (2) 0.14 (0.15)	[-0.08; 1.46] 0.69 (0.47) 285 [-0.22; 1.61] 0.69 (0.47) 285 [-0.51; 1.90]	.32
-0.05 (0.14) [-0.32; 0.22] -0.05 (0.14) [-0.40; 0.30]	0.69 (0.47) 285 [-0.22; 1.61] 0.69 (0.47) 285 [-0.51; 1.90]	
[-0.32; 0.22] -0.05 (0.14) [-0.40; 0.30]	[-0.22; 1.61] 0.69 (0.47) 285 [-0.51; 1.90]	
-0.05 (0.14) [-0.40; 0.30]	0.69 (0.47) 285	.32
21] [-0.40; 0.30]	[-0.51; 1.90]	.32
(2) 0.14 (0.15)		
	2.93 (2.27) 158	.86
66] [-0.10; 0.39]	[-0.81; 6.67]	
(2) 0.14 (0.15)	2.93 (2.27) 158	.86
18] [-0.15; 0.44]	[-1.53; 7.39]	
(2) 0.14 (0.15)	2.93 (2.27) 158	.86
15] [-0.24; 0.53]	[-2.93; 8.78]	
-0.17 (0.16)	0.42 (0.32) 153	.74
9] [-0.43; 0.09]	[-0.10; 0.94]	
-0.17 (0.16)		.74
2] [-0.48; 0.14]	[-0.20; 1.04]	
-0.17 (0.16)	0.42 (0.32) 153	.74
6] [-0.57; 0.23]		
	()	15
5] [-0.49; -0.01		
-0.25 (0.18)	0.23 (0.20) 95.9	15
3] [-0.56; 0.07]	[-0.11; 0.56]	
	0.23 (0.20) 95.9	15
1] [-0.71; 0.21]		
-0.05 (0.19)	0.86 (0.82) 136	.88
19] [-0.37; 0.27]	[-0.48; 2.21]	
, ,	` /	.88
89] [-0.43; 0.33]	[-0.74; 2.47]	
		.88
26] [-0.54; 0.45]	[-1.24; 2.97]	
1 1 1 3 3 3 3 3 3 3 3 3 3 3 3 3 3 3 3 3	66] [-0.10; 0.39] 82) 0.14 (0.15) 18] [-0.15; 0.44] 82) 0.14 (0.15) 15] [-0.24; 0.53] 4) -0.17 (0.16) 9] [-0.43; 0.09] 4) -0.17 (0.16) 2] [-0.48; 0.14] 4) -0.17 (0.16) 6] [-0.57; 0.23] 8) -0.25 (0.18) 6] [-0.49; -0.01] 8] -0.25 (0.18) 1] [-0.71; 0.21] 8] -0.05 (0.19) 19] [-0.37; 0.27] 8] -0.05 (0.19) 89] [-0.43; 0.33] -0.05 (0.19)	66] [-0.10; 0.39] [-0.81; 6.67] 32) 0.14 (0.15) 2.93 (2.27) 158. 18] [-0.15; 0.44] [-1.53; 7.39] 32. 32) 0.14 (0.15) 2.93 (2.27) 158. 15] [-0.24; 0.53] [-2.93; 8.78] 158. 4) -0.17 (0.16) 0.42 (0.32) 153. 9] [-0.43; 0.09] [-0.10; 0.94] 153. 4) -0.17 (0.16) 0.42 (0.32) 153. 2] [-0.48; 0.14] [-0.20; 1.04] 153. 4) -0.17 (0.16) 0.42 (0.32) 153. 6] [-0.57; 0.23] [-0.39; 1.23] 153. 8) -0.25 (0.18) 0.23 (0.20) 95.9 5] [-0.49; -0.01] [-0.03; 0.49] 95.9 3] [-0.56; 0.07] [-0.11; 0.56] 95.9 3] [-0.56; 0.07] [-0.11; 0.56] 95.9 1] [-0.71; 0.21] [-0.27; 0.72] 95.9 3) -0.05 (0.19) 0.86 (0.82) 136.

Table 6: Univariate point process parameter (PP) estimates.

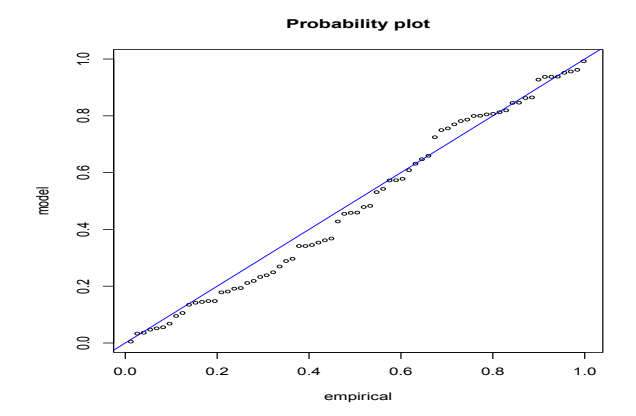
3.18 Return levels

Table 5 displays the estimates of the return levels and their corresponding confidence intervals (in parentheses) for the markets. Since the return series in this study was re-scaled by multiplying by 100, the return levels interpretations are presented in percentages. For the Brazilian IBOV market, a maximum loss of 7.41% is expected once every 2 years, 8% once every 5 years, 8.44% once every 10 years, 8.86% once every 20 years, and 9.39% once every 50 years. For the Russian IMOEX market, a maximum loss of 16.87% is expected once every 2 years, 20.03% once every 5 years, 22.72% once every 10 years, 25.69% once every 20 years, and 30.10% once every 50 years are shown in the table. For the Indian NIFTY market, a maximum loss of 6.76% is expected once every 2 years, 7.08% once every 5 years, 7.29% once every 10 years, 7.47% once every 20 years, and 7.69% once every 50 years. For the Chinese SHCOMP, a maximum loss of 6.03% is expected once every 2 years, 6.19% once every 5 years, 6.29% once every 10 years, 6.37% once every 20 years, and 6.46% once every 50 years. Lastly, for the South African JALSH market, a maximum loss of 9.12% is expected once every 2 years, 9.86% once every 5 years, 10.41% once every 10 years, 10.93% once every 20 years, and 11.60% once every 50 years.

3.19 Univariate analysis: Point process

The procedure used for the GPD fit under the CEV model is also applied to the univariate analysis of the point process model. To enable appropriate comparison between the two models, the same threshold is used. Hence, for the parameter estimation of the point process model, the Poisson process will be fitted to the same declustered exceedances (i.e. the cluster-maxima) used for the GPD fit.





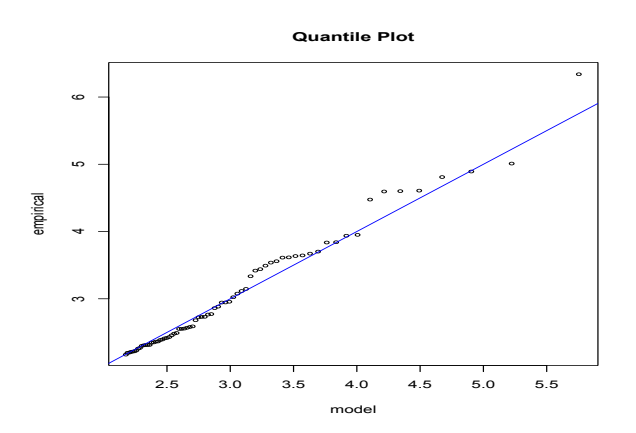


Fig. 9: IBOV: Point process diagnostic plots.

3.20 Point process fit to cluster-maxima

As it is under the GPD parameters estimation, the 71, 45, 39, 23, and 36 cluster-maxima observations are the collective risk levels in the Brazilian, Russian, Indian, Chinese and South African markets respectively at the chosen thresholds. Each collection represents different magnitudes or levels of risk in that particular market. The point process is fitted to each market's cluster-maxima and the results in Table 6 are obtained. The standard errors of the estimates are enclosed in parentheses while the confidence intervals are in the brackets. The results obtained for the shape parameter ξ are very similar to that of the GPD estimation.

Like the GDP fit, for the Russian IMOEX market, the positive estimate ($\xi = 0.14$) of the shape parameter as shown in the table for the point process indicates a fat-tailed distribution and it reflects concavity [](Coles, 2001). The shape parameter estimates for the Brazilian, Indian, Chinese and South African markets are $\xi = -0.05$, $\xi = -0.17$, $\xi = -0.25$, and $\xi = -0.05$ respectively. The shape parameters' negative estimates indicate a short tailed distribution that reflects convexity (Coles, 2001). However, since the values of the confidence intervals of the estimated shape parameters at the three confidence levels in the table are from negative to positive including zero, a formal hypothesis test is conducted in Section 3.21 using the likelihood ratio (LR) and the modified likelihood ratio (LR_{**}) tests to ascertain if $\xi = 0$ or otherwise.

3.21 Formal hypothesis test

From the outcomes in Table 7, at the 1%, 5% and 10% levels of significance, the values of the likelihood ratio (LR) and the modified likelihood ratio (LR_{**}) tests are greater than the critical values. Hence, the null hypothesis of $\xi=0$ is rejected in the five markets in favour of the alternative that $\xi\neq0$. For the Russian IMOEX market, the positive shape parameter estimate ($\hat{\xi}=0.14$) as shown in the table corresponds to an unbounded distribution. Therefore, the risk in the Russian IMOEX market using the point process approach can be described by the Fréchet-Pareto class of distributions (see Beirlant et. al [?]).

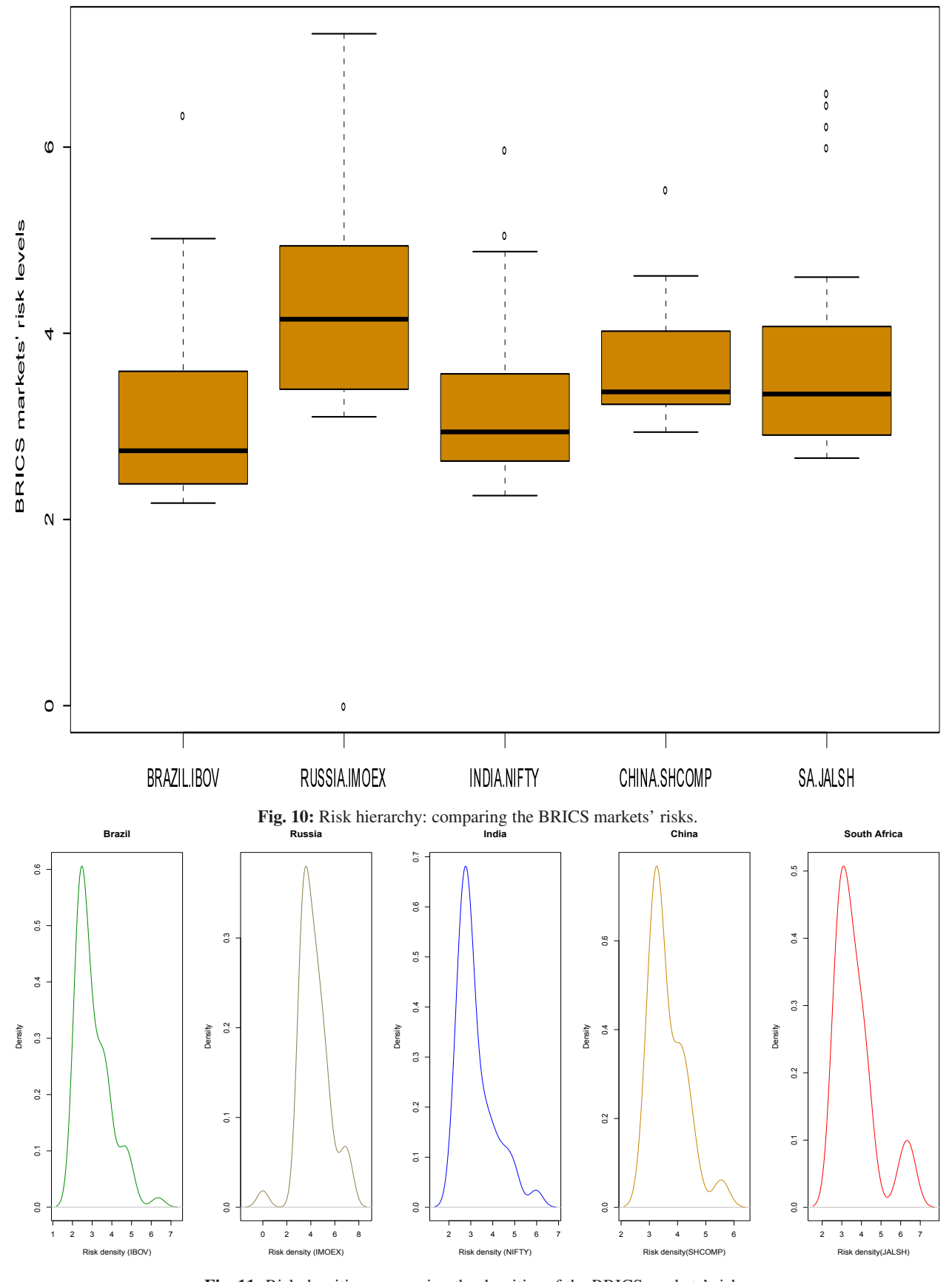
The negative shape parameter ($\xi < 0$) estimates for the Brazilian, Indian, Chinese and South African markets in the table correspond to a bounded distribution, i.e. a Weibull domain of attraction. Hence, the risks in these four markets using the point process approach can be modelled by the Weibull class of distributions, with a finite upper bound.

3.22 Point process diagnostic plots and return levels

As shown in Figure 9, and Figures 19, 20, 21 and 22 in the Appendix, the data points in the diagnostic probability plot and quantile plot of the point process of the Brazilian IBOV, Russian IMOEX, Indian NIFTY, Chinese SHCOMP and South African JALSH markets respectively are close to the 45° lines, except for the lone outlier at the extremes of the quantile plots of the Russian IMOEX market in Figure 19 and the Chinese SHCOMP market in Figure 21. Hence, the point process fit is satisfactory.

Table 8 shows the point process return level estimates and their corresponding confidence intervals (in parentheses) for the IBOV, IMOEX, NIFTY, SHCOMP and JALSH indices respectively. The return level estimates from the point process are similar to that of the GPD in Table 5.





 $\textbf{Fig. 11:} \ \textbf{Risk densities: comparing the densities of the BRICS markets' risks.}$

Table 7. Electrifold ratio test for 11 35 estimates.							
	w	ξ	LR	CV	LR_{**}	CV	
	71	-0.05	570.64	10%: 2.706	548.14	10%: 2.706	
Brazilian IBOV				5%: 3.841		5%: 3.841	
				1%: 6.635		1%: 6.635	
	45	0.14	317.72	10%: 2.706	297.95	10%: 2.706	
Russian IMOEX				5%: 3.841		5%: 3.841	
				1%: 6.635		1%: 6.635	
	39	-0.17	307.48	10%: 2.706	285.40	10%: 2.706	
Indian NIFTY				5%: 3.841		5%: 3.841	
				1%: 6.635		1%: 6.635	
	23	-0.25	191.90	10%: 2.706	168.54	10%: 2.706	
Chinese SHCOMP				5%: 3.841		5%: 3.841	
				1%: 6.635		1%: 6.635	
	36	-0.05	273.76	10%: 2.706	252.47	10%: 2.706	
S/African JALSH				5%: 3.841		5%: 3.841	
				1%: 6.635		1%: 6.635	

Table 7: Likelihood ratio test for PP's ξ estimates.

w is the number of cluster-maxima observations and CV is the critical value.

IBOV 2-year 5-year 10-year 20-year 50-year 8.847.19 7.93 8.41 9.38 R_g 90% CI (4.79; 9.58)(4.56; 11.30)(4.32; 12.49)(4.02; 13.67)(3.54; 15.23)95% CI (3.92; 11.95)(3.54; 13.28)(4.33; 10.04)(3.10; 14.59)(2.42; 16.35)99% CI (3.43; 10.94)(2.66; 13.21)(2.01; 14.80)(1.29; 16.39)(0.24; 18.53)**IMOEX** 5-year 10-year 20-year 50-year 2-year $\widehat{R_g}$ 15.84 19.65 22.53 25.60 30.08 90% CI (5.93; 25.75)(3.72; 35.57)(1.33; 43.73)(-1.81; 53.01)(-7.37; 67.53)95% CI (4.04; 27.65)(0.67; 38.62)(-2.73; 47.78)(-7.06; 58.26) (-14.55; 74.71)(-5.29; 44.58)99% CI (0.33; 31.36)(-10.65; 55.71)(-17.31; 68.51)(-28.55; 88.71) NIFTY 2-year 5-year 10-year 20-year 50-year $\widehat{R_g}$ 6.64 7.04 7.27 7.47 7.68 90% CI (4.75; 8.52)(4.60; 9.49)(4.45; 10.09)(4.29; 10.64)(4.06; 11.31)95% CI (4.39; 8.88)(4.13; 9.96)(3.91; 10.63)(3.68; 11.25)(3.36; 12.00)(3.21; 10.87) 99% CI (3.69; 9.59)(2.85; 11.69)(2.49; 12.44)(2.01; 13.36)SHCOMP 2-year 10-year 20-year 50-year 5-year R_g 5.97 6.17 6.28 6.36 6.45 90% CI (4.78; 7.15) (4.70; 7.64)(4.63; 7.93)(4.55; 8.17)(4.45; 8.45)95% CI (4.43; 7.51)(4.26; 8.08)(4.14; 8.42)(4.01; 8.71)(3.86; 9.05)99% CI (3.72; 8.21) (3.38; 8.96)(3.15; 9.41)(2.93; 9.80)(2.66; 10.25)JALSH 2-year 5-year 10-year 20-year 50-year 8.84 9.78 10.37 10.92 11.60 R_g 90% CI (4.75; 8.52)(4.60; 9.49)(4.45; 10.09)(4.29; 10.64)(4.06; 11.31) 95% CI (4.13; 9.96)(3.91; 10.63)(3.68; 11.25)(3.36; 12.00)(4.39; 8.88)99% CI (3.69; 9.59)(3.21; 10.87)(2.85; 11.69)(2.49; 12.44)(2.01; 13.36)

Table 8: Point process return level (R_g) estimates.

4 Conclusions

4.1 Comparing the performance of the CEV's GPD and PP models

To start with, the likelihood estimated shape parameters for both the CEV's GPD and point process models are the same in the five BRICS equity market. However, since the values of the confidence intervals range from negative to positive



and cover zero, a formal hypothesis test was conducted. The outcome of the test showed that under the GPD model, the risks in the BRICS markets can all be modelled by the Gumbel class of distributions. Under the point process approach however, the risk in the Russian equity market can be modelled by the Fréchet-Pareto class of distributions, while the risks in the Brazilian, Indian, Chinese and South African equity markets can be modelled by the Weibul class of distributions. Furthermore, the diagnostics checks carried out using various diagnostics plots for the two models and the goodness of fit tests for the GPD show that the models' fits are adequately satisfactory. In addition, the return level estimates are nearly the same for the two models. In conclusion, the likelihood estimation of the two models are approximately the same, but the GPD has fewer parameters to compute than the point process.

4.2 Risk hierarchy: comparing the markets' equity risks

The magnitudes or levels of risk in the BRICS equity markets are compared using the boxplot in Figure 10. The plot displays the risk hierarchy from the highest to the lowest, with their associated densities in Figure 11. Based on the relative spread (or variability) of each box in Figure 10, it can be observed that the Russian IMOEX market has the highest level of risk, followed by the South African (SA) JALSH market, then the Chinese SHCOMP, Brazilian IBOV and Indian NIFTY markets respectively. This finding shows that the Russian IMOEX market is the most risk-prone, while the least risky is the Indian NIFTY market, with the remaining three markets in between them. The Brazilian IBOV market is however very slightly higher than the Indian NIFTY market in risk level as shown in the plot. High investment risk may either yield potential high returns as a reward or a huge loss to an investor.

The boxplots further show the shapes of the risk in each of the markets based on the concentration of the clustermaxima observations on the scale. From Figure 10, the distribution of the risk observations in the IBOV, NIFTY, SHCOMP and JALSH markets are all skewed to the right, while the IMOEX market is near-symmetric.

Acknowledgement

The authors are grateful to the numerous people for helpful comments on this paper.

Conflict of interest

The authors declare that they have no conflict of interest.

References

- [1] H. Tian, The BRICS and the G20, China & World Economy 24, 111-126 (2016).
- [2] S. Sashi, Cracks in BRICs: A sectoral financial balances analysis and implications for macroeconomic policy, Theoretical and Applied Economics. Asociatia Generala a Economistilor din Romania - AGER, Autumn 3, 53-78 (2016).
- [3] G. Galloppo, V. Paimanova, and M. Aliano, Volatility and Liquidity in Eastern Europe Financial Markets under Efficiency and Transparency Conditions. Economics and Sociology 8, 70-92 (2015).
- [4] R. Engle, GARCH 101: the use of ARCH/GARCH models in applied econometrics. Journal of Economic Perspectives 15, 157-168 (2001).
- [5] M.A.M. Al-Janabi, Risk Management in Trading and Investment Portfolios: An optimisation Algorithm for Maximum Riskbudgeting Threshold. Journal of Emerging Market Finance, SAGE Publications 11, 189-229 (2012).
- [6] M. Karmakar and S. Paul, Intraday risk management in International stock markets: A conditional EVT approach. International Review of Financial Analysis, (2015), http://dx.doi.org/10.1016/j.irfa.2015.11.008
- [7] T.G. Bali, An extreme value approach to estimating volatility and value at risk. Journal of Business 76, 83-108 (2003).
- [8] N. Taleb, Fooled by Randomness: The hidden role of chance in the markets and life. New York, N.Y. Random House, (2007).
- [9] B. Mandelbrot, The Variation of Certain Speculative Prices. The Journal of Business, The University of Chicago Press 36, 394-419 (1963).
- [10] R. de Jesus, E. Ortiz, and A. Cabello, Long run peso/dollar exchange rates and extreme value behavior: at risk modeling. The North American Journal of Economics and Finance 24, 139-152 (2013).
- [11] P.A. Santos, I.F. Alves, and S. Hammoudeh, High quantiles estimation with quasi-port and dpot: An application tovalue-at-risk for financial variables. The North American Journal of Economics and Finance 26, 487-496 (2013).
- [12] M. McAleer, J.A. Jimenez-Martin, and T. Perez-Amaral, Has the Basel accord improved risk management during the global financial crisis?. The North American Journal of Economics and Finance 26, 250-265 (2013).



- [13] R. Herrera and B. Schipp, Statistics of extreme events in risk management: The impact of the subprime and global financial crisis on the German stock market, North American Journal of Economics and Finance **29**, 218-238 (2014).
- [14] A.J. McNeil and R. Frey, Estimation of Tail Related Risk Measure for Heteroscedastic Financial Time Series: An Extreme Value Approach. J. Empir. Financ. 7, 271-300 (2000).
- [15] V. Marimoutou, B. Raggad, and A. Trabelsi, Extreme value theory and value at risk: application to oil market. Energy Economics 31, 519-530 (2009).
- [16] A. Ghorbel and A. Trabelsi, Predictive performance of conditional extreme value theory in value-at-risk estimation. International Journal of Monetary Economics and Finance 1, 121-148 (2008).
- [17] J. Cotter, Varying the VaR for unconditional and conditional environments. Journal of International Money and Finance 26, 1338-1354 (2007).
- [18] T.G. Bali and S.N. Neftci, Disturbing extremal behavior of spot price dynamics. Journal of Empirical Finance 10, 455-477 (2003).
- [19] M. Karmakar and G.K. Shukla, Managing extreme risk in some major stock markets: An extreme value approach. International Review of Economics and Finance 35, 1-25 (2015).
- [20] R.L. Smith, Statistics of extremes, with applications in environment, insurance, and finance. Monographs on Statistics and Applied Probability, 54-60 (2003).
- [21] A.T. Ergun and J. Jun, Time-varying higher-order conditional moments and forecasting intraday VaR and expected shortfall. Quarterly Review of Economics and Finance **50**, 264-272 (2010).
- [22] V. Chavez-Demoulin and J.A. McGill, High-frequency financial data modeling using Hawkes processes. Journal of Banking & Finance **36**, 3415-3426 (2012).
- [23] P. Embrechts, C. Klüppelberg and T. Mikosch, Modeling Extremal Events for Insurance and Finance. Springer, New York, (1997).
- [24] D. Ardia, H. Lennart, and C. Nienke, Stock index returns' density prediction using GARCH models: Frequentist or Bayesian estimation?. aeris CAPITAL AG, Tinbergen and Econometric Institutes, Erasmus University Rotterdam, The Netherlands MPRA Paper No. 28259, (2011), https://mpra.ub.uni-muenchen.de/28259/.
- [25] Y. Hong, Y. Liu, and S. Wang, Granger causality in risk and detection of extreme risk spillover between financial markets, Journal of Econometrics **150**, 271-287 (2009).
- [26] R.A. Fisher and L.H.C. Tippett, Limiting forms of the frequency distribution of the largest and smallest member of a sample. Proc. Camb. Phil. Soc. 24, 180-190 (1928), Bibcode:1928PCPS...24..180F, https://doi.org/10.1017/S0305004100015681
- [27] B.V. Gnedenko, Sur la distribution limite du terme maximum d'une serie aleatoire. Annals of Mathematics 44, 423-453 (1943), doi:10.2307/1968974, JSTOR 1968974.
- [28] M. Gilli and E. Kellezi, An Application of extreme value theory for measuring financial risk. Comput Econ 27, 1-23 (2006).
- [29] S. Coles, An Introduction to Statistical Modelling of Extreme Values, 81-156 (2001).
- [30] J. Danielsson, P. Hartmann, and C. de Vries, The cost of conservatism, RISK 11, 101-103 (1998).
- [31] P. Embrechts, S. Resnick, and G. Samorodnitsky, Living on the Edge. Risk Magazine 11, 96-100 (1998).
- [32] H. Southworth, J.E. Heffernan and P.D. Metcalfe, texmex: Statistical modelling of extreme values. R package version 2.4, (2017).
- [33] C.A.T. Ferro, Statistical Methods for Clusters of Extreme Values. Lancaster University, (2003).
- [34] Y. Hu and C. Scarrott, Evmix: An R package for extreme value mixture modelling, threshold estimation and boundary corrected kernel density estimation, (2018).
- [35] C. Scarrott and A. MacDonald, A review of extreme value threshold estimation and uncertainty quantification. REVSTAT Statistical Journal 10, 33-60 (2012).
- [36] J.E. Heffernan and H. Southworth, texmex: Statistical modelling of extreme values, R package version 2.1., (2013).
- [37] E. Castillo, S. Ali, A.S. Hadi, N. Balakrishnan, and J.M. Sarabia, Extreme Value and Related Models with Applications in Engineering and Science. Wiley, New York 241-250, (2005).
- [38] J.R.M. Hosking, Testing whether the shape parameter is zero in the generalized extreme-value distribution. Biometrika **71**, 367-374 (1984).
- [39] S. Buuren and K. Groothuis-Oudshoorn, MICE: Multivariate imputation by chained equations in R. Journal of Statistical Software 45, 1-67 (2011).
- [40] H. Yang, Extreme value mixture modelling with simulation study and applications in finance and insurance, (2013).
- [41] C.A.T. Ferro and J. Segers, Inference for clusters of extreme values. Journal of the Royal Statistical Society. Series B (Statistical Methodology) 65, 545-556 (2003).
- [42] S. Fukutome, M.A. Liniger and M. Süveges, Automatic threshold and run parameter selection: a climatology for extreme hourly precipitation in Switzerland. Theor Appl Climatol 120, 403-416 (2015).
- [43] R.L. Smith, Extreme value analysis of environmental time series: An Application to Trend Detection in Ground-Level Ozone, Statistical Science 4, 367-377 (1989).
- [44] M.A. Ribatet, A User's Guide to the POT Package (Version 1.0) 12, 69-71, (2006). http://cran.r-project.org/.



Appendix

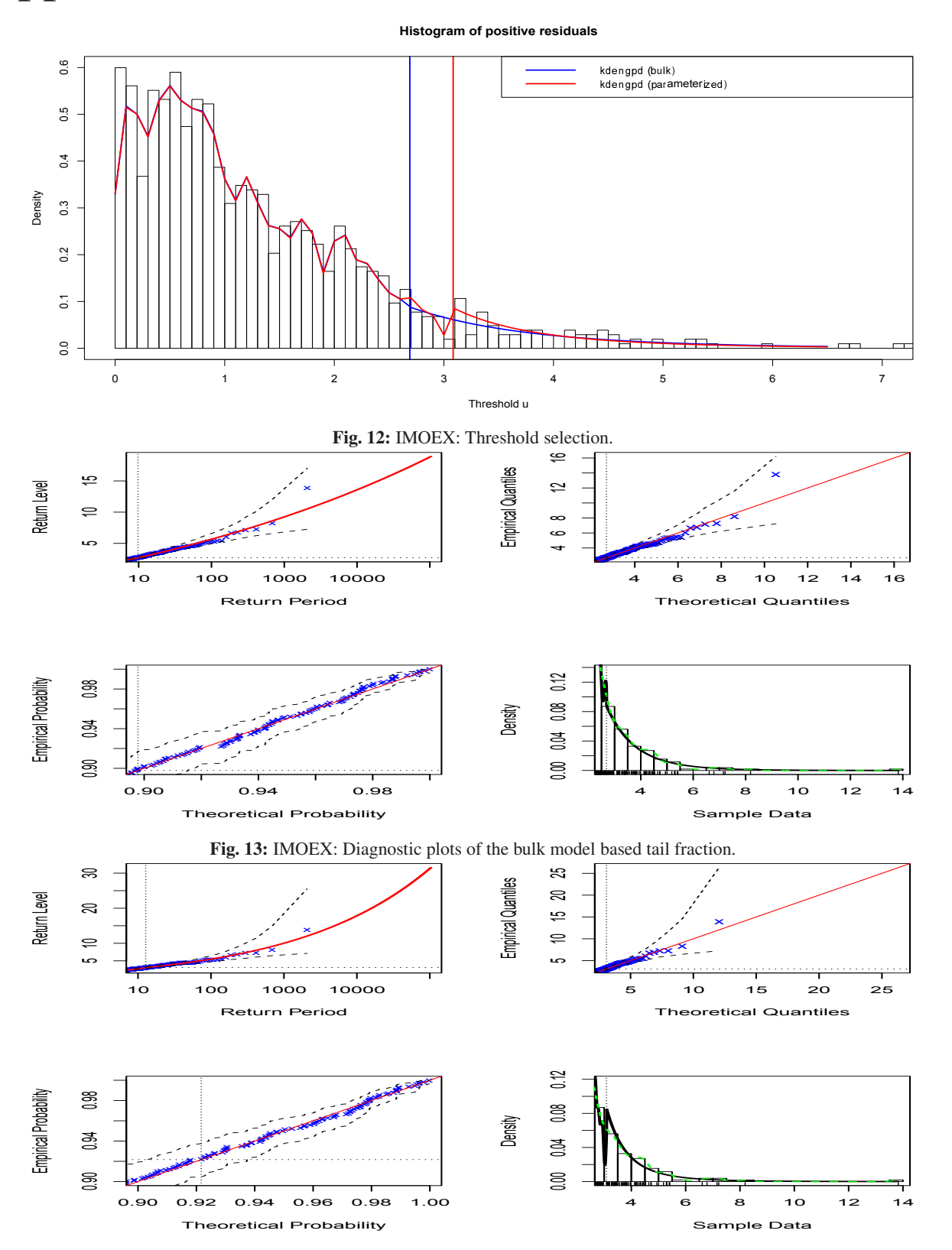


Fig. 14: IMOEX: Diagnostic plots of the parameterized tail fraction.



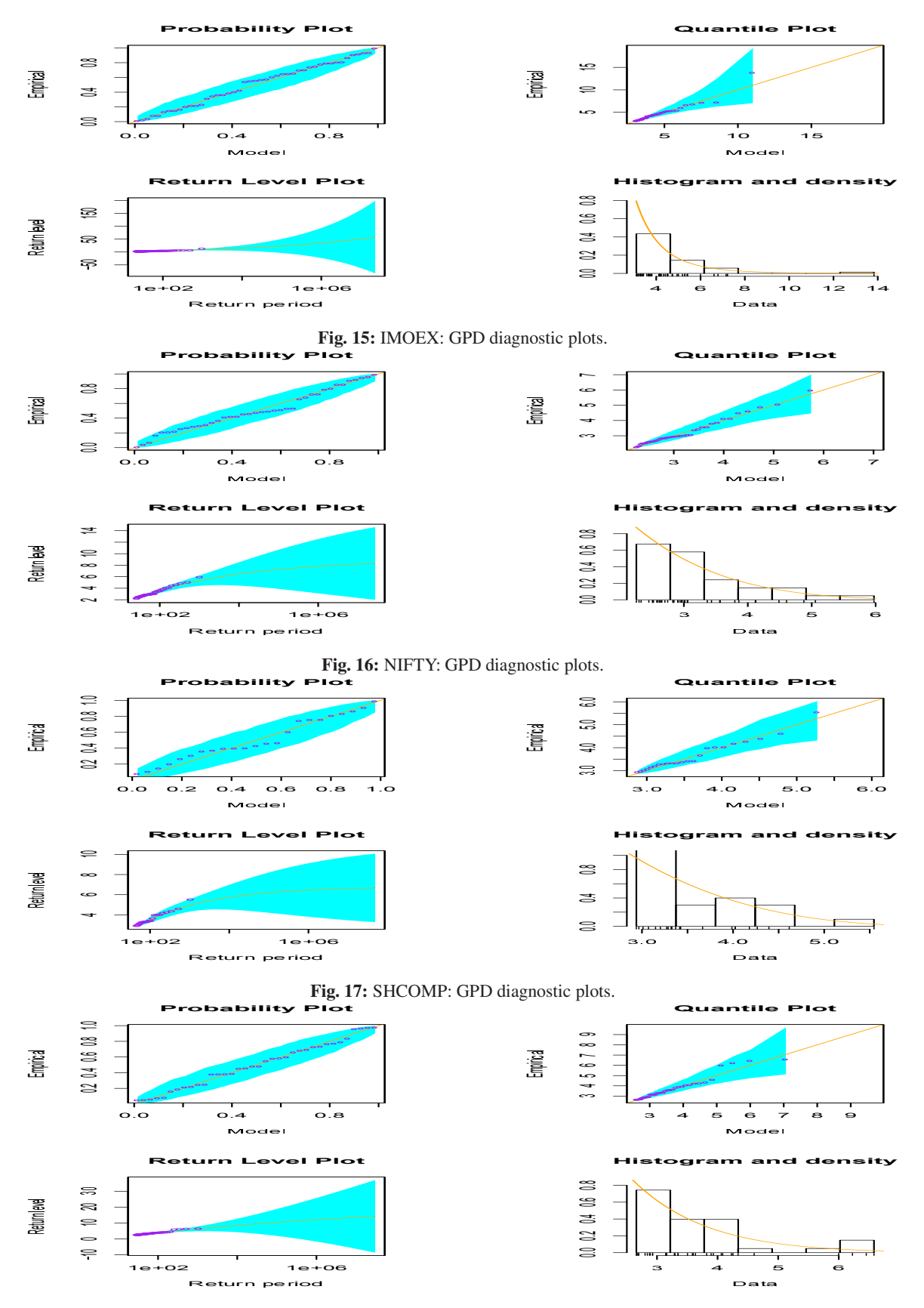


Fig. 18: JALSH: GPD diagnostic plots.



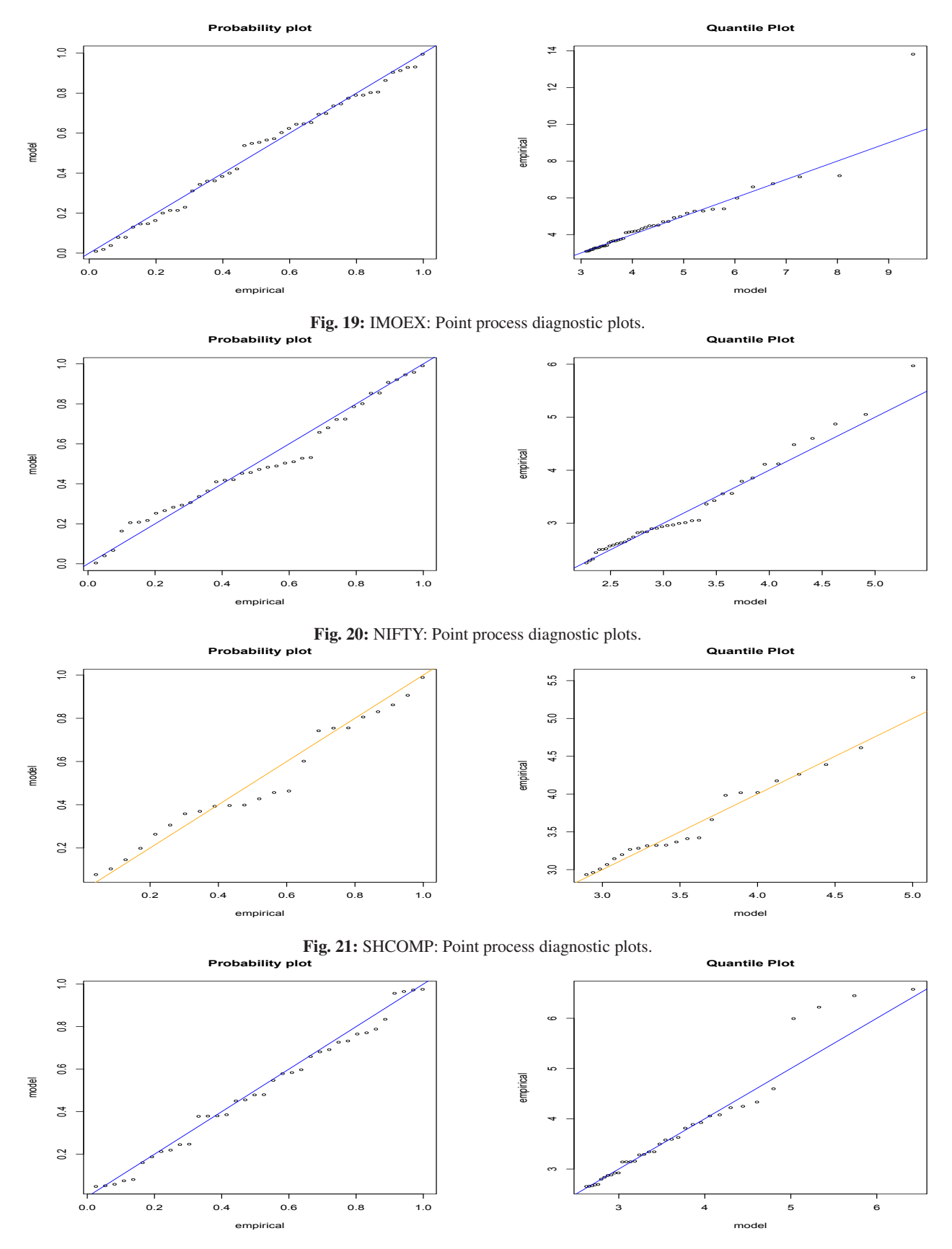


Fig. 22: JALSH: Point process diagnostic plots.